



HAL
open science

The geometric spectrum of lava domes and spines

Amy Myers, Claire Harnett, Eoghan Holohan, Thomas Walter, Michael Heap

► **To cite this version:**

Amy Myers, Claire Harnett, Eoghan Holohan, Thomas Walter, Michael Heap. The geometric spectrum of lava domes and spines. *Volcanica*, 2024, 7 (2), pp.665-684. 10.30909/vol.07.02.665684. hal-04743988

HAL Id: hal-04743988

<https://hal.science/hal-04743988v1>

Submitted on 19 Oct 2024

HAL is a multi-disciplinary open access archive for the deposit and dissemination of scientific research documents, whether they are published or not. The documents may come from teaching and research institutions in France or abroad, or from public or private research centers.

L'archive ouverte pluridisciplinaire **HAL**, est destinée au dépôt et à la diffusion de documents scientifiques de niveau recherche, publiés ou non, émanant des établissements d'enseignement et de recherche français ou étrangers, des laboratoires publics ou privés.



Distributed under a Creative Commons Attribution 4.0 International License

The geometric spectrum of lava domes and spines: new perspectives from analysis of the Morphology of Viscous Extrusions (MoVE) global dataset

 Amy J. Myers^{*α},  Claire E. Harnett^α,  Eoghan P. Holohan^α,  Thomas R. Walter^β, and
 Michael J. Heap^{γ,δ}

^α UCD School of Earth Sciences, University College Dublin, Belfield, Dublin, Ireland.

^β GFZ German Research Centre for Geosciences, Telegrafenberg, 14473 Potsdam, Germany.

^γ Université de Strasbourg, CNRS, Institut Terre et Environnement de Strasbourg, UMR 7063, 5 rue Descartes, Strasbourg F-67084, France.

^δ Institut Universitaire de France (IUF), Paris, France.

ABSTRACT

Extrusion of viscous lava produces domes and spines, collapses of which pose a significant local hazard. Understanding extrusion processes and probabilistic hazard estimation require comprehensive datasets of geometric parameters. We introduce Morphology of Viscous Extrusions (MoVE), a collation of 323 observations of height and width from 80 extrusions at 46 volcanoes globally with compositions spanning basaltic through rhyolitic. Filtering this dataset for sample size, age, and time series overrepresentation reduces the composition range to basaltic-andesitic through dacitic, for which we do not identify a statistically significant effect of composition on extrusion geometry. Young (<200 yr) basaltic or rhyolitic domes are either rare or underrepresented globally. Five well-resolved time series highlight various height-width evolutions and scales possible during growth. Extrusion heights and widths are well-estimated by a Weibull distribution and scale according to a truncated power law; this can guide parameter values used in probabilistic hazard models of collapse-associated pyroclastic density currents.

KEYWORDS: Dome growth; Height; Width; Aspect ratio; Viscous extrusion; Power law.

1 INTRODUCTION

The flow behaviour of extruded lava is largely dependent on its effective viscosity [Swanson and Holcomb 1990]. Lava extrusions display a range of geometries that can be characterised most simplistically in terms of their aspect ratio (i.e. height to width). Lava domes or lava spines typically form from magma that is too viscous to flow far from the vent after effusive extrusion and have been observed at over 225 volcanoes globally [Calder et al. 2015; Ogburn et al. 2015]. Lava spines are often thought of as relatively high aspect ratio members of a broad spectrum, with lava flows representing low aspect ratio extrusions. Viscous, high aspect ratio lava extrusions are commonly unstable, and their collapse can yield hot pyroclastic density currents that inundate areas far from the point of collapse [Miller 1994; Watts et al. 2002].

The simplest examples of lava domes observed in nature are approximately circular when viewed from above and have steeply inclined sides and a flat top surface, much like a truncated cone [Hutchison et al. 2013]. Lava domes grow over variable timescales, and it can be a number of years before collapse is triggered (e.g. Sinabung, Indonesia [Carr et al. 2022]). In contrast, lava spines are short-lived columnar extrusions prone to collapse soon after formation due to their higher aspect ratio, and therefore greater instability [Griffiths 2000; Rhodes et al. 2018]. Reasons for this variation in extrusion geometry and behaviour include the viscosity of the melt [e.g. Závada et al. 2009], magma porosity and crystallinity [e.g. Heap et al. 2016], eruption rates [e.g. Fink and Griffiths 1998],

extrusion of a solidified plug in the upper conduit [e.g. Iverson 2008; Zorn et al. 2019], the presence of remnant domes [e.g. Závada et al. 2009], existing crater glaciers [e.g. Walder et al. 2007], and the topography of the extrusion surface which may include pre-existing craters [e.g. Ashwell et al. 2018; Moussallam et al. 2021].

Lava domes can grow via two modes; endogenous growth occurs when fresh material is injected into the core of a lava dome causing it to inflate, whereas exogenous growth is characterised by extrusion of lava at the surface. Lava domes growing endogenously consist of a hot ductile core encased in a cooler carapace and surrounded by steep slopes of brittle talus, the relative volume of each component varying during the course of an eruption [Wadge et al. 2009]. Lateral spreading of the ductile interior can occur under the influence of gravity, causing the talus slopes to steepen and the dome front to advance by way of material spalling [e.g. Voight and Elsworth 2000]. Lava spines are one possible result of exogenous growth, forming from stiffer extruded lava with greater resistance to gravitational spreading. Processes that can cause a lava to stiffen include degassing-induced crystallisation [e.g. Sparks et al. 2000], cooling in the upper conduit [e.g. Giordano et al. 2008], and a decreased extrusion rate [e.g. Fink and Griffiths 1998; Rutherford 2008]. Spine growth commonly accompanies the onset and early stages of dome growth (e.g. Mount St. Helens, USA [Major et al. 2009] and Volcán de Colima, Mexico [Savov et al. 2008]), but has also been recorded in the final phases of lava dome growth (e.g. Augustine, USA [Coombs et al. 2010]) and in the later stages of analogue experiments [e.g. Zorn et al. 2020]. As composition classifications are

*✉ myers.amyj@outlook.com

based on silica content, and the viscosity of a melt increases as a function of silica content [e.g. Swanson et al. 1987; Rogers 2015], we hypothesise that extrusions with high aspect ratios will have compositions associated with high silica content.

To understand processes of extrusion and facilitate probabilistic estimation of hazard, comprehensive datasets of geometric parameters are needed. In this study, we collated recorded height, width, emplacement timeframe, observation timeframe, and composition from published literature into a dataset titled Morphology of Viscous Extrusions (MoVE) to enable systematic analysis and characterisation of these parameters. We characterised the frequency distributions of, and the relationships between, extrusion height, width, and aspect ratio. We also statistically analysed the potential roles of composition and age on reported extrusion geometries. Lastly, we explored the benefit of analysing time series acquisitions with good temporal resolution on the order of days for use in understanding lava dome growth patterns.

2 METHODS

2.1 Data collation

In this study, we collated previously published data to better characterise the geometric variation of viscous lava extrusions that are classified in the source publication as either lava domes or lava spines. The data required for inclusion in MoVE are estimated height and width measurements and extrusion composition; we also collected data pertaining to extrusion volume, estimated magma viscosity, ascent rate, and crystallinity where possible. Composition data are primarily sourced from the summary profile and bulletin records hosted by the Global Volcanism Program [GVP 2023], but if extrusion composition (as opposed to the composition of the volcanic system as a whole) was not available, this data was instead taken from literature. In all cases, reference publications are fully recorded. In addition, we opted to exclude any records with a low level of confidence that both the height and width measurements represent the same feature at the same time. The result is a geographically diverse dataset with 323 entries from approximately 80 extrusions recorded at 46 volcanoes globally (Figure 1A). Their compositions range from basaltic through to rhyolitic (Figure 1B), the most common being dacitic (42 %) or andesitic (32 %). Mount St. Helens (23 %), Volcán de Colima (12 %), Soufrière St. Vincent, Saint Vincent and the Grenadines (8 %), and Mount Unzen, Japan (8 %), have the greatest number of observations. In total, the eight most sampled sites account for 68 % of the observations (Figure 1C).

Available data on extrusion dimensions mostly concern point-measurements. These measurements provide individual snapshots of the dimensions, often without context as to the exact timing within an eruption and do not offer information on how extrusion proceeds through time. Our knowledge of viscous extrusion geometry is therefore geographically thorough but often lacks the temporal dimension. In contrast, a time series record ideally needs to have good temporal resolution, meaning data were recorded frequently and at regular intervals where possible. Time series datasets are improving

with the use of modern technologies, such as remote sensing instrumentation and more sophisticated post-processing approaches. One recent example comes from Merapi, Indonesia, where an array of remotely programmable monitoring stations has been established to relay real-time observations of lava dome activity to the observatory [Kelfoun et al. 2021]. Consequently, we also include and examine data from the five best-constrained time series of viscous extrusion growth contained in MoVE (from Mount St. Helens, Mount Unzen, Volcán de Colima, Soufrière St. Vincent, and Pinatubo).

The information contained in MoVE originates from a variety of sources, including but not limited to journal articles, observatory reports, activity bulletins, photographic atlases, book chapters, and the current version of the DomeHaz database [Ogburn et al. 2012; 2015]. Many of these sources contain data summarised from earlier publications. Where it has been possible to access the original source, we have included both references in MoVE. A complete list of references can be found in MoVE*, which will remain open access to facilitate continued recording of variables including extrusion geometry, volume, viscosity, ascent rate, and crystallinity. We further hope that this repository can be used to validate future numerical and analogue model results.

2.2 Estimated geometric parameters of extrusions in previous works

Given the range of sources used in this study, the methods used by the original authors to collect the raw data are also varied. Here we present an overview of the primary geometric data collection methods as documented in the source publications.

One method for obtaining height and width estimates of viscous extrusions is from geological maps. This technique is best suited to old lava domes that are no longer active and have therefore been mapped in reasonably high detail. Examples of extrusion dimensions obtained this way include measurements from the Maroa Volcanic Centre located in New Zealand [Blake 1990] and the Coso Volcanic Field located in the USA [Duffield and Bacon 1981]. In the examples cited by Blake [1990], extrusion width was back-calculated from aerial extent assuming simple circular base geometry. Therefore, this methodology is most applicable to axisymmetric lava domes with clearly defined outlines.

More recent monitoring techniques have made use of uncrewed aerial vehicles (UAVs) and satellite acquisitions. The creation of multiple DEMs across an eruption allows us to identify regions of material accumulation or loss and to estimate related volume changes [e.g. Schilling et al. 2008; Diefenbach et al. 2013; Thiele et al. 2017; Vallejo et al. 2024]. However, georeferencing the resulting DEM can be difficult in dynamic environments such as volcanic craters as identifiable features may be displaced or destroyed. In addition, volcanic activity such as degassing and ash venting, may obscure the crater and prevent image acquisition.

To overcome these limitations, satellite imagery presents a promising alternative. The remote sensing capabilities of synthetic aperture radar satellites, such as the TerraSAR-X satel-

*<https://thegithub.org/resources/4988>

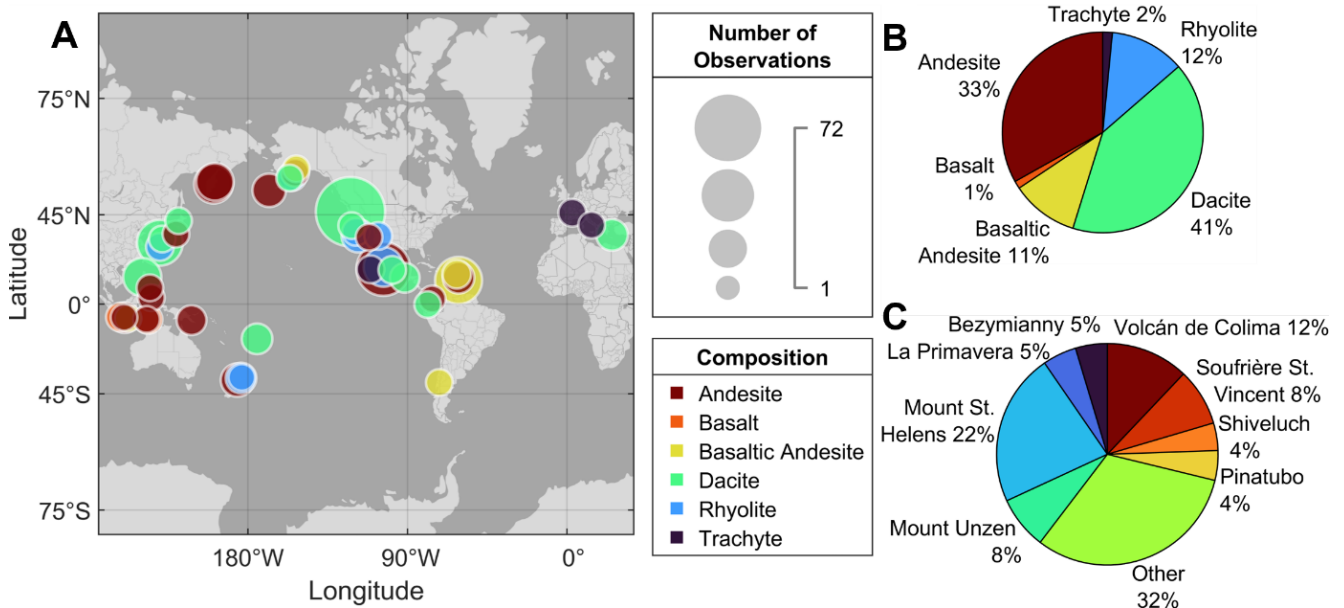


Figure 1: [A] Map showing the geographical distribution of volcanoes contained in MoVE. The size of the circles corresponds to the number of observations for that site, and the colour indicates composition; [B] pie chart showing the proportion of observations as a function of composition; [C] pie chart showing the proportion of observations attributed to the different volcanoes featured in the dataset.

lite [e.g. Wang et al. 2015; Walter et al. 2019; Ordoñez et al. 2022], allow images to be obtained even when an eruption cloud is present. Since the orbit of a satellite is regular and predictable, it is also possible to obtain time series imagery at regular intervals. For example, Walter et al. [2019] present a time series record of lava dome growth at Volcán de Colima that spans four weeks and has a spatial resolution of 2 m. These acquisitions supplement the results of optical imagery, providing one of the best visual time series records of lava dome growth readily accessible in the literature.

Nakada and Shimizu [2013] used theodolite measurements to record lava dome growth at Mount Unzen from December 1993 to March 1995 on a Mimatsu diagram; this is an efficient way of recording the growth evolution of an extrusion as a series of stacked profiles. Such diagrams were also used at Shiveluch, Russia [Zharinov and Demyanchuk 2008] through a combination of land-based and aerial imaging techniques.

For this study, we assume that all methods outlined here provide equally robust measurements of extrusion height and width and that classification as a lava dome or lava spine as recorded in the source publication is accurate and reliable.

2.3 Statistical analysis

We used the software IBM SPSS Statistics v.27 to conduct a statistical analysis of the dataset, with all tests conducted at the 95 % confidence interval ($\alpha = 0.05$). Given the uneven sample sizes across the six compositional groups ($n_{\text{Bas}} = 4$; $n_{\text{BasAnd}} = 35$; $n_{\text{And}} = 107$; $n_{\text{Dac}} = 133$; $n_{\text{Trach}} = 5$; $n_{\text{Rhy}} = 39$), we first tested whether the height, width, and aspect ratio data in each compositional group are normally distributed using the Kolmogorov-Smirnov and Shapiro-Wilk tests. These tests assess the degree of difference between the

data distribution and a normal distribution, with a significant result suggesting that a normal distribution does not fit the dataset. Since the assumption of normality was violated across all compositional groups, we continued analysis using a non-parametric approach. We used a ranked Kruskal-Wallis (K-W) test to assess whether the difference in the mean rank of height, width, and aspect ratio across the compositional groups was statistically significant. To perform this test, every value of the chosen parameter was assigned a rank, with a minimum value of N . After ranking, the data were sorted according to composition, and the test statistic, H_{df} , was calculated using Equation 1, where R_i is the sum of the ranks assigned to datapoints in compositional group i , and n_i is the sample size of group i :

$$H_{df} = \frac{12}{N(N+1)} \sum_{i=1}^k \frac{R_i^2}{n_i} - 3(N+1). \quad (1)$$

H_{df} was then compared to the Chi-squared distribution, where the degrees of freedom equal the number of compositional groups minus one. If the variability in the dataset is consistent with expected random variability in nature, then the mean rank will be similar across the compositional groups, and H_{df} will have an associated significance $p > 0.05$. In the event of a significant H_{df} value being returned ($p < 0.05$), pairwise tests were carried out to identify which pairs of compositional groups showed statistically significant differences. If the K-W test returned a non-significant result, no further analysis was carried out. We applied a series of filters to the dataset to account for low sample size within certain compositional groups ($n_{\text{Int1}} = 314$), extrusion age ($n_{\text{Int2}} = 265$), and overrepresentation of volcanoes with time series records

($n_{\text{Final}} = 185$) and repeated the statistical analysis using the procedure outlined above.

3 RESULTS

3.1 Overview of dataset

The dataset presented here contains 323 entries of extrusion height, width, and magma composition (Figure 1), with further information (where available) hosted in the full online version of MoVE*. The structure of MoVE includes columns for spine length, extrusion volume, extrusion rate, viscosity, density, and crystal content. The completeness of these fields is varied as we only filled in values that were reported in the same publication as the height and width data. The most complete additional field is estimated volume; 118 (37 %) of the 323 entries have additional volume estimates. The least complete field is density; only seven (2 %) of the 323 entries have this information recorded. The completeness of the extrusion rate, viscosity, and crystallinity fields are 7 % (21 values), 7 % (24 values), and 7 % (24 values), respectively. Just under half (41 %) of entries include data in at least one additional field, and the number of filled additional fields per measurement entry has an arithmetic mean of 1.46. The observation time-frame field was completed as fully as possible based on the source literature. A number of entries have uncertain eruption and/or observation dates (16 %); these are recorded with an estimated age taken from the literature. Precision of the reported date varies from day (59 %) to month (7 %) to year (19 %).

3.2 Geometric spectrum of domes and spines

Histograms of the height, width, and aspect ratio data are provided in Figure 2. Approximately 50 % of the height values are below 100 m, indicating a strong skew toward lower height values (Figure 2A). The maximum height recorded in the dataset is 800 m (Pinatubo [Newhall et al. 1996]). The histogram of width also shows a strong skew toward lower width values, with a well sampled population up to ~2500 m (Figure 2B). The maximum width recorded in the dataset is 5000 m (O'Leary Peak, USA [Green and Short 1971]). The histogram of aspect ratio, calculated as height/width, is dominated by values less than 0.5 (Figure 2C). There is a moderate skew toward lower aspect ratio values, with a maximum aspect ratio in the dataset of 3.16 (Mont Pelée, Martinique [Lacroix 1904]).

Figure 3 shows height as a function of width for all entries in the MoVE. The designation as either a lava spine (red triangles) or a lava dome (blue circles) is based on the description in the source publication. There is an overall positive relationship between the height and width of viscous extrusions. Of the 292 reported lava domes, 238 (82 %) have an aspect ratio < 0.4. Of the 29 reported spines, 23 (79 %) have aspect ratios > 0.9.

Following the recommendation outlined in Blake [1990], the data are also displayed on a log-log plot (Figure 4). We observe a clear positive correlation between the logarithmic height and logarithmic width of viscous extrusions, with a moderate de-

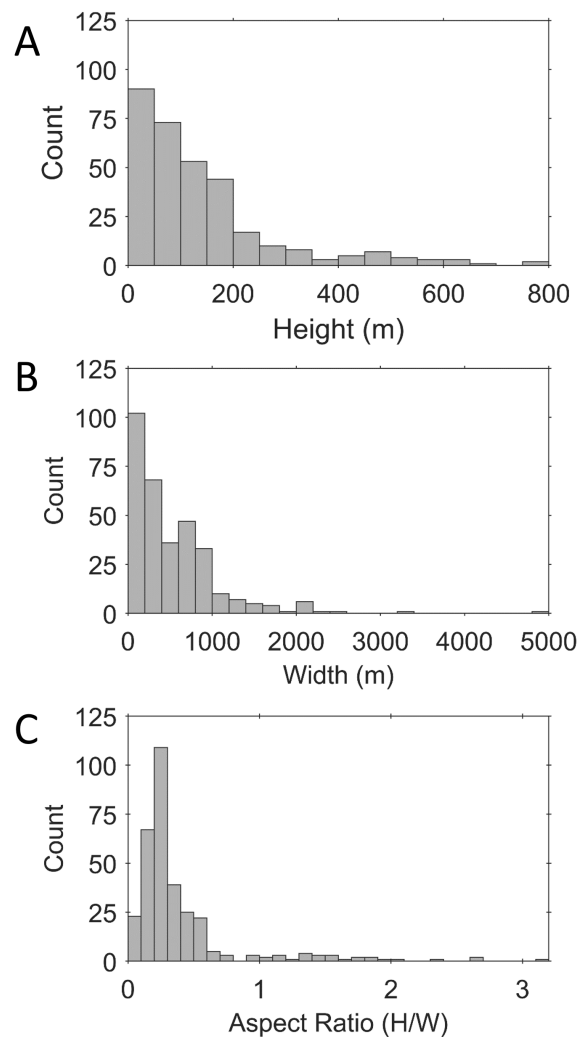


Figure 2: Histograms of [A] reported height; [B] reported width; and [C] aspect ratio for viscous extrusions, as found in published literature. Histograms of extrusion height, width, and aspect ratio for the data in MoVE at all stages of the filtering process can be found in Supplementary Material 1 Figure S1.

gree of overlap between features previously characterised as lava domes or lava spines. This overlap is most apparent for aspect ratios of 0.4–0.6.

3.3 Correlations between extrusion composition, age, and dimensions

We further interrogate the dataset by considering the effect that magma composition may have on the possible size of viscous extrusions, as composition is the most complete additional field in the dataset. Figure 5 shows height as a function of width of the recorded extrusions, coloured by magma composition in line with Figure 1B. Extrusions of dacite and andesite are found for a wide range of aspect ratios, with no clear distinction between the two compositions. The rhyolite extrusions diverge from the other compositions, with 46 % of extrusions having an aspect ratio < 0.1. To test whether composition is a primary control on extrusion geometry, we carried out a systematic statistical analysis on the full dataset.

* <https://theghub.org/resources/4988>

Table 1: Summary of the data in MoVE, sorted by country and volcano, showing the number of observations collected and the extrusion composition according to the Global Volcanism Program 2023. Names are taken from the relevant GVP [2023] profile, for the full list of sources refer to the online dataset. Compositions listed here represent the most common composition recorded in the dataset for each volcano. For extrusion-specific composition data, we refer the reader to the online dataset.

Country	Volcano	Observations	Composition
Chile	Carrán-Los Venados	1	Basaltic Andesite
Colombia	Nevado del Huila	1	Andesite
Ecuador	Guagua Pichincha	1	Dacite
France	Chaîne des Puys	2	Trachyte
	Pelée	5	Andesite
Greece	Santorini	6	Dacite
Guatemala	Santa María	4	Dacite
	Awu	1	Andesite
Indonesia	Galunggung	3	Basalt
	Iliwerung	3	Basalt
	Kelud	1	Basaltic Andesite
	Lewotobi	1	Andesite
	Merapi	5	Andesite
	Sumbing	1	Andesite
Italy	Ischia	1	Trachyte
	Abu	1	Dacite
Japan	Kikai	2	Rhyolite
	Nikko-Shiranesan	1	Andesite
	Toya	1	Dacite
	Unzendake	25	Dacite
Mexico	Bárcena	2	Trachyte
	Sierra la Primavera	16	Rhyolite
	Popocatepetl	2	Dacite
	Colima	38	Andesite
Montserrat	Soufrière Hills	3	Basaltic Andesite
New Zealand	Maroa	5	Rhyolite
	Okataina	1	Rhyolite
	Taranaki	8	Andesite
Papua New Guinea	Lamington	2	Andesite
Philippines	Camiguin	1	Andesite
	Pinatubo	14	Dacite
Russia	Bezymianny	14	Andesite
	Sheveluch	12	Andesite
Saint Vincent	Soufrière St. Vincent	27	Basaltic Andesite
Tonga	Lateiki	5	Dacite
	Augustine	2	Andesite
	Bogoslof	8	Andesite
	Coso Volcanic Field	8	Rhyolite
	Lassen Volcanic Centre	1	Dacite
	St. Helens	72	Dacite
	Novarupta	3	Rhyolite
	Mono-Inyo Craters	2	Rhyolite
	San Francisco Volcanic Field	1	Andesite
	Valles Caldera	2	Rhyolite
	Redoubt	1	Basaltic Andesite
	Ukinrek Maars	1	Dacite

Here we report the results of a series of statistical tests performed to investigate the possible relationship between composition and extrusion geometry. In summary, we first tested the full dataset of 323 measurements and found that

the height, width, and aspect ratio of an extrusion is dependent on composition. We then filtered the dataset to obtain (a) groups with sufficient sample size to be statistically powerful (dataset $n_{\text{Int1}} = 314$ after removal of $n_{\text{Bas}} = 4$ and $n_{\text{Trach}} = 5$),

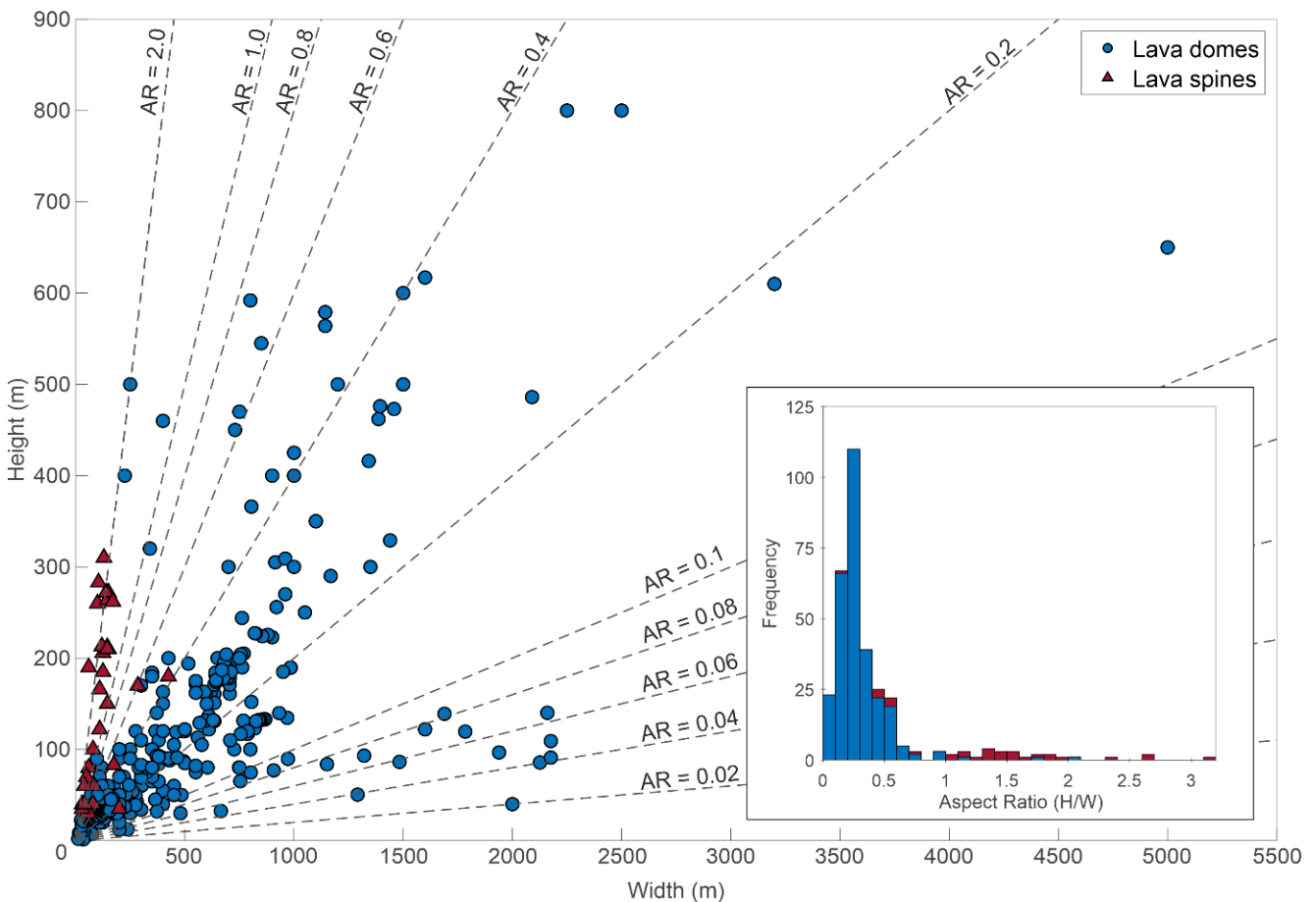


Figure 3: Plot of lava dome (circles) and lava spine (triangles) height and width data. Designation as a lava dome or lava spine is based on the information reported in the source publication. Dashed lines are added to show lines of equal aspect ratio.

(b) extrusions with ages < 250 years across all compositions ($n_{\text{Int}2} = 265$ after removal of the remaining rhyolites due to their now small sample size), and (c) extrusions that are point measurements rather than part of a well-resolved time series record ($n_{\text{Final}} = 185$). We repeated the analysis on the filtered dataset and found that the height, width, and aspect ratio of an extrusion is independent of composition. The results are summarised in Table 2.

Since the data do not follow a normal distribution, we opted to use the Kruskal-Wallis test for independent samples. We first tested the null hypothesis that the heights, widths, and aspect ratios of viscous extrusions are independent of magma composition. We found a statistically significant difference in the mean rank for extrusion height ($H_5 = 22.843$, $p < 0.001$), extrusion width ($H_5 = 55.743$, $p < 0.001$), and aspect ratio ($H_5 = 91.570$, $p < 0.001$). Given the small number of basaltic and trachytic extrusions reported in the dataset and the subsequent low statistical power of these groups, we removed these data and repeated the analysis. We again found a statistically significant difference in the mean ranks for extrusion height ($H_3 = 14.112$, $p = 0.003$), extrusion width ($H_3 = 53.970$, $p < 0.001$), and aspect ratio ($H_3 = 86.702$, $p < 0.001$).

The pairwise comparison conducted after calculation of H_{df} repeatedly identified the rhyolite group as showing a statistical difference in mean rank in both datasets (n_{Total} and $n_{\text{Int}1}$).

Based on this observation and supported by the distribution of the rhyolite data in Figure 5, we investigated whether there could be a confounding factor underlying the rhyolite data that could account for the statistically significant variability. Of the 39 observations from rhyolitic extrusions in the original dataset, only five showed confirmed ages corresponding to recent activity (defined here as ≤ 250 years). The other 34 observations referred to older (age > 250 years) extrusions that are likely to have experienced a significant degree of weathering, the effects of which may be captured in the recorded geometric measurements. For this reason, we removed all observations (of any composition) where the time between activity and measurement > 250 years. This reduced the sample sizes of the andesite (from $n = 107$ to $n = 105$), dacite (from $n = 133$ to $n = 125$), and rhyolite (from $n = 39$ to $n = 5$) groups. Only five entries remained in the rhyolite group, so we excluded these data due to their low statistical power. We repeated the K-W test on the twice-filtered dataset ($n_{\text{Int}2} = 265$) and found a statistically significant difference between the mean ranks for extrusion height ($H_2 = 13.740$, $p = 0.001$), extrusion width ($H_2 = 21.908$, $p < 0.001$), and aspect ratio ($H_2 = 21.169$, $p < 0.001$).

Lastly, we considered whether the inclusion of time series data acts as an additional confounding factor. There are five well-resolved time series records of lava dome growth in the

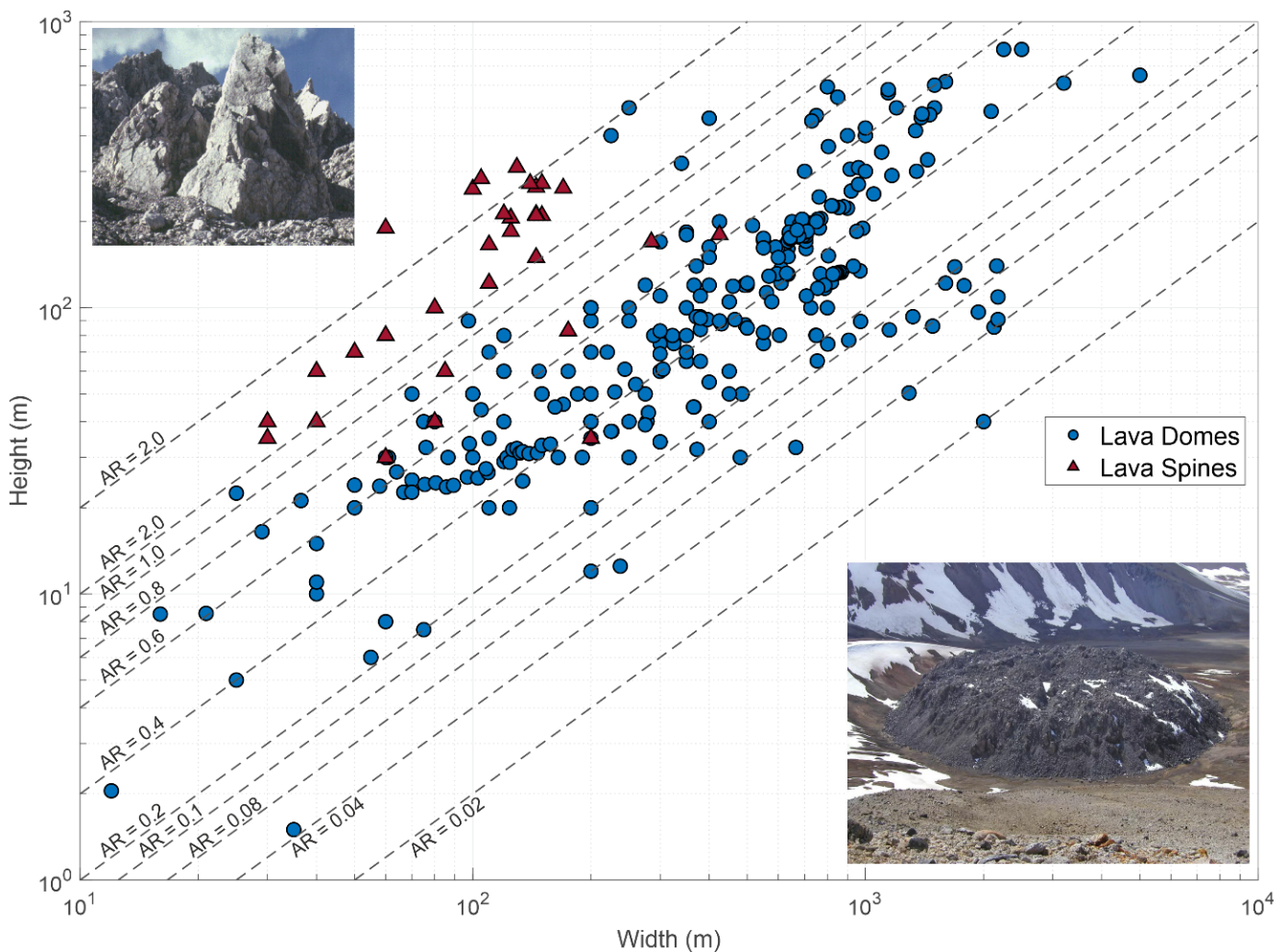


Figure 4: Log-log plot of height and width of measured viscous extrusions. Characterisation as either a lava dome or lava spine is taken from the source publication. Extrusions classified by previous researchers as lava domes dominate at aspect ratios < 0.6 , and those classified as lava spines at aspect ratios > 0.6 . Dashed lines represent lines of equal aspect ratio. Photographs show typical geometries for lava domes (Novarupta, USA; USGS) and lava spines (Santiaguito, Guatemala; Bill Rose).

Table 2: Summary of H values and associated p -values calculated during statistical analysis of the role of composition on the published height, width, and aspect ratio of viscous extrusions. A p -value < 0.05 indicates a statistically significant difference is detected between the mean rank of two or more compositional groups. Subscript numbers denote the degrees of freedom for that analysis.

	Height	Width	Aspect ratio	Interpretation
Full dataset ($n_{\text{Total}} = 323$)	$H_5 = 22.843$ $p < 0.001$	$H_5 = 55.743$ $p < 0.001$	$H_5 = 91.570$ $p < 0.001$	Geometry is influenced by composition
Sample size filtering ($n_{\text{Int1}} = 314$)	$H_3 = 14.112$ $p = 0.003$	$H_3 = 53.970$ $p < 0.001$	$H_3 = 86.702$ $p < 0.001$	Geometry is influenced by composition
Age filtering ($n_{\text{Int2}} = 265$)	$H_2 = 13.740$ $p = 0.001$	$H_2 = 21.908$ $p < 0.001$	$H_2 = 21.169$ $p < 0.001$	Geometry is influenced by composition
Time series filtering ($n_{\text{Final}} = 185$)	$H_2 = 0.285$ $p = 0.867$	$H_2 = 2.529$ $p = 0.282$	$H_2 = 5.178$ $p = 0.075$	Composition has no statistically significant effect on geometry

dataset, and these observations comprise a significant proportion of the sample size across the compositional groups (26 % of the andesite, 28 % of the dacite, and 46 % of the basaltic andesite data are attributed to time series records). The remaining data are point measurements that represent

extrusions at an unknown time after onset of extrusion. Time series data, therefore, could have introduced bias to the statistical analysis by incorporating data that misrepresents results of natural sampling. Therefore, we further filtered the dataset to generate a final dataset ($n_{\text{Final}} = 185$), shown in

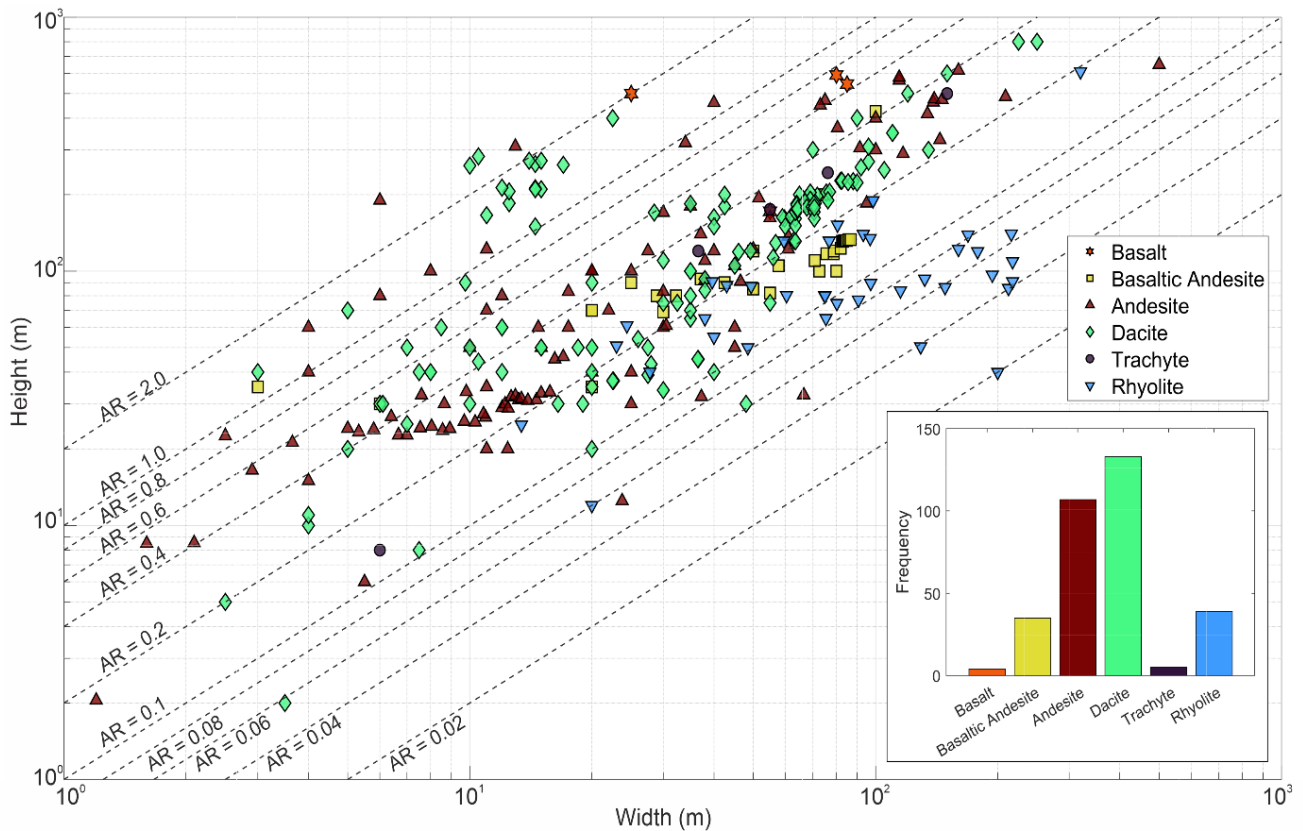


Figure 5: Log-log plot of reported extrusion heights and widths, coloured by composition. 63 % of the data fall between aspect ratios of 0.2–0.8. Exceptions include the high aspect ratio structures largely corresponding to spines and the wide but low rhyolite extrusions (blue triangles). The inset histogram shows the number of observations in each compositional group, coloured according to Figure 1B.

Figure 6. We again investigated the null hypothesis that the geometry of viscous extrusions is independent of magma composition. A Kruskal-Wallis test for independent samples in this case returned a non-significant difference in the mean ranks of extrusion height ($H_2 = 0.285$, $p = 0.867$), extrusion width ($H_2 = 2.529$, $p = 0.282$), and aspect ratio ($H_2 = 5.178$, $p = 0.075$). The non-significant result therefore accepts the null hypothesis and finds that the geometry of viscous extrusions is indeed independent of composition for the compositions remaining in the filtered dataset (basaltic andesite, andesite, and dacite).

3.4 Growth of viscous extrusions through time

The duration and measurement intervals of the five time series records included in this dataset are summarised in Table 3, and the related temporal evolutions of the geometric parameters (height, width, and aspect ratio) during growth are illustrated in Figure 7. We first normalised each time series to its final height, width, and aspect ratio values to identify common trends that might otherwise be obscured due to the different length and time scales of growth of each lava dome. Thus, if the final value is not also the maximum value, then normalised dimensions can have values > 1 .

Figure 7A shows height evolution through time, which is generally characterised by an initial short period of rapid in-

crease, before the rate of increase slows and the height reaches an approximate steady state. The width evolution (Figure 7B) is more varied with Mount Unzen showing very little change in width, whilst the width of the Volcán de Colima dome shows an approximately linear increase with time. Figure 7C shows the aspect ratio as a function of time. Both Volcán de Colima and Soufrière St. Vincent exhibit an easily identifiable peak aspect ratio (0.58 and 0.50 respectively) during early growth, before reaching an approximate steady state. The curves for both Mount St. Helens and Pinatubo show a more modest increase in aspect ratio early in the time series and reach a steady state earlier than Volcán de Colima and Soufrière St. Vincent. The aspect ratio of the Mount Unzen lava dome ranges between 0.21 and 0.28 which suggests this time series misses the early stages of lava dome growth and instead records growth of a pre-established lava dome, an interpretation that is further supported by the initial height (132 m) and width (630 m) measurements recorded.

4 DISCUSSION

In this study we present MOVE, a new dataset that collates existing lava dome and lava spine geometry measurements from associated literature. We found that the distributions of height, width, and aspect ratio show a moderate to strong degree of positive skew. Plotting the data on log-log axes showed a re-

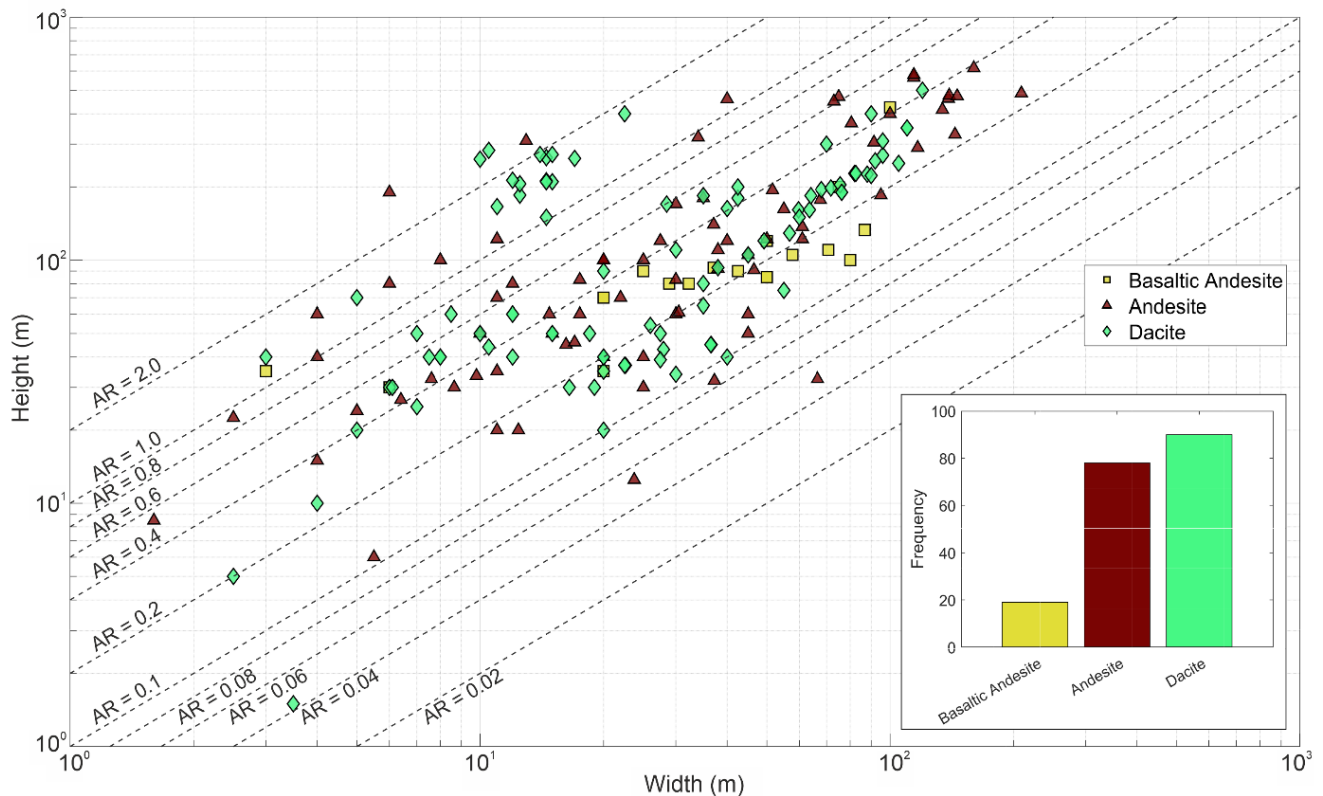


Figure 6: Log-log plot of reported extrusion heights and widths for the entries contained in the final filtered dataset ($n_{\text{Final}} = 185$). 81% of the data fall between aspect ratios of 0.1–0.6. The exceptions are the high aspect ratio structures largely corresponding to spines. The inset histogram shows the number of observations in each compositional group, coloured according to Figure 1B.

Table 3: Summary of the time series data, including the timescales of data collection and the number of measurements in each time series record.

Volcano	Observation period	Time (days)	Number of measurements	Average interval (days)	Citation
Mount St. Helens	13/06/1980 – 07/02/1983	842	11	76.5	Swanson et al. [1987]
Volcán de Colima	14/02/2013 – 13/03/2013	28	27	1.04	Walter et al. [2019]
Pinatubo	14/07/1992 – 30/10/1992	109	10	10.9	Daag et al. [1996]
Soufrière St. Vincent	07/05/1979 – 02/10/1979	149	16	9.32	Huppert et al. [1982]
Mount Unzen	30/12/1993 – 08/03/1995	434	14	31	Nakada and Shimizu [2013]

gion of overlap (at aspect ratios of 0.4–0.6) between extrusions previously described as lava domes or lava spines. When considering composition, we found that extrusions with rhyolitic compositions showed a greater average width compared to that of other compositional groups. Our analysis confirmed that rhyolitic lava domes were responsible for much of the statistically significant variation observed between each compositional group, but that this variation may be linked to a confounding factor of extrusion age. Normalised time series records of lava dome growth from five volcanoes showed a general growth trend of a rapid initial increase in height, and to a lesser extent width; this was reflected in higher aspect ratios earlier in the time series. During continued extrusion, the rate of increase in both height and width decreases, as

reflected in the aspect ratio settling to a more consistent and lower value.

4.1 Characterising the distributions of height, width, and aspect ratio

We demonstrated that recorded heights, widths, and aspect ratios of extrusions contained in MoVE are not normally distributed. We applied predicted models of three common distributions to the heights, widths, and aspect ratios in our dataset (Figure 8). In all instances, the Weibull distribution (blue curve) provided the best fit to the dataset, whilst the half-normal distribution (green curve) consistently showed the worst fit.

The Weibull distribution is characterised by three parameters, namely a scale (η), shape (β), and threshold (γ) param-

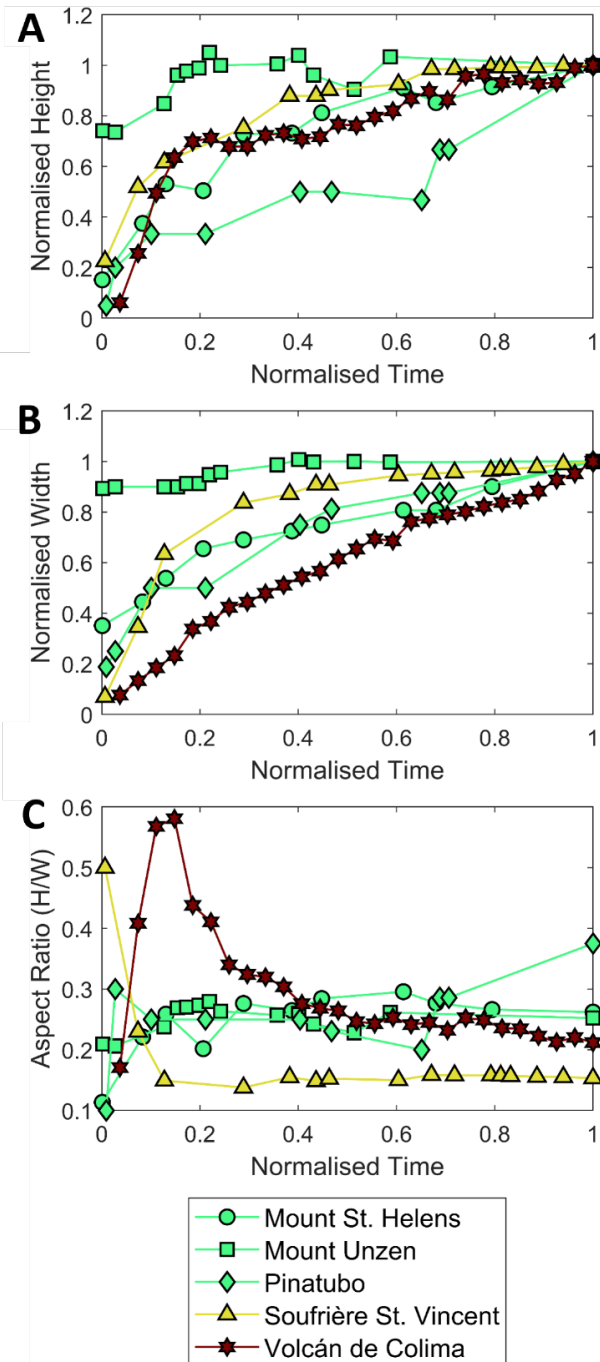


Figure 7: Time series plots of viscous extrusion dimensions coloured for composition according to Figure 1B [A] Evolution of height with time. [B] Evolution of width with time. [C] Evolution of the aspect ratio (height, H , divided by width, W) with time. All variables have been normalised to assist comparison of growth patterns measured over different time scales. The time series shown here are for the sites and time periods given in Table 3. The extrusion was characterised and recorded as a lava dome throughout the time series period. (Data sources: Huppert et al. [1982], Swanson et al. [1987], Daag et al. [1996], Nakada and Shimizu [2013], and Walter et al. [2019]).

eter. In this case, we set γ equal to zero since the form of a

viscous extrusion means it will never have a negative height or width. This simplifies the distribution to a two-parameter Weibull distribution, where η corresponds to the 63.2 percentile and β determines the direction of skew. We find that extrusion heights and extrusion widths are best described by two-parameter Weibull distributions where the value of β ranges from 1.04 to 1.17. Weibull distributions are increasingly being used to describe observations in the field of Earth sciences, particularly in volcanology. Recent examples include describing the variability observed in tephra deposit thickness [Daggitt et al. 2014], estimating the likelihood of eruption as a function of repose time [Wang and Bebbington 2012], describing how the size of magmatic dykes are distributed [Krumbholz et al. 2014], and numerical modelling of rock heterogeneity and the subsequent effect on the stability of lava domes [Heap et al. 2023]. The main implication of dimension data, especially extrusion widths, following a two-parameter Weibull distribution is that there is a lower bound to the width, i.e. lava dome geometry is not entirely scale-independent. As discussed below, this possibly relates to the fundamental physical control of conduit diameter and bulk magma viscosity on magma ascent.

4.2 The relationships between extrusion height, width, and age

Figure 5 and Figure 8 hint at a possible power law relationship governing the growth of lava domes. Evidence for this, as outlined by Glen [2023], includes the positively skewed distribution of height and width measurements (Figure 3), as well as the approximate linear trend between the logarithmic heights and widths (Figure 5). Power law distributions are not unusual in nature; examples in the geosciences include the magnitude of earthquakes [Corral and González 2019], the size distribution of fractures [Corral and González 2019], the size distribution of gas bubbles in magma [Blower et al. 2003], runout distance of pyroclastic density currents with respect to discharge rates [Roche et al. 2021], and magma viscosity relative to depth [Sparks 1997]. Furthermore, both Huppert et al. [1982] and Blake [1990] previously proposed a power law relationship to describe the dimensions of various lava domes, including Soufrière St. Vincent, La Primavera (Mexico), and the Coso Volcanic Field (USA).

The power law relationship suggested by Blake [1990] was applied to lava domes that have been inactive for an extended time period. We have shown that measurements of height and width taken from old lava domes are associated with much larger inaccuracies, which we hypothesise relate to erosion and possible differences in susceptibility driven by magma composition. If a lava dome is inactive for an extended period, erosion can increase the rate of degradation and promote landsliding of gravitationally unstable talus piles. Material will be removed from the upper portions of the lava dome and deposited on the slopes, which increases the width and decreases the height of the extrusion. We suggest this is the cause for variability in the data from old rhyolitic lava domes in Figure 5, which diverge from the rest of the dataset towards comparatively wider and lower geometries. Additionally, the deposition of material on the slopes of the lava dome may ob-

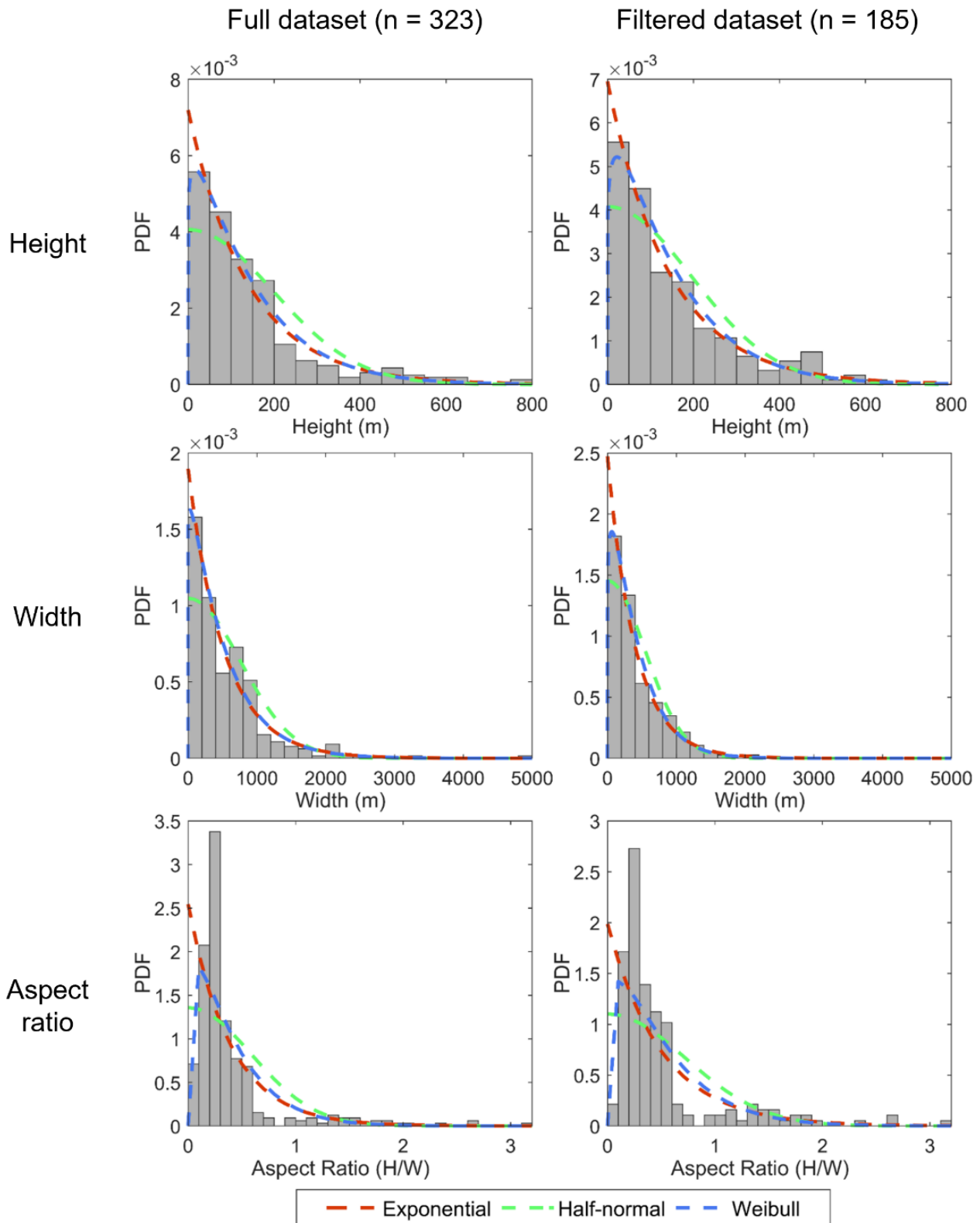


Figure 8: Probability density functions (PDF) of height, width, and aspect ratio for the full ($n_{\text{Total}} = 323$) and final filtered ($n_{\text{Final}} = 185$) datasets. Curves of the predicted PDF for three common models (exponential, half-normal, and Weibull) are shown; in all instances the Weibull distribution provides the best fit to the data. PDFs and associated predicted model fits for extrusion height, width, and aspect ratio of all datasets can be found in [Supplementary Material 1 Figure S2](#).

sure the interface between neighbouring lava domes, causing a lava dome complex to be misinterpreted as a single large lava dome.

Further evidence supporting the presence of a power law relationship governing extrusion geometry is seen in cumulative frequency curves for each parameter on logarithmic axes. Rather than the linear trend expected if a simple power law governed the possible size of an extrusion, the data instead follow a negative exponential curve (Supplementary Material 1 Figure S3). Each curve, however, features a linear section that covers the middle portion of the dataset. This is indicative of a truncated power law which occurs when a parameter cannot take values at one or both extremes of the distribution [Corral and González 2019].

We next used the full and final filtered datasets to investigate the relationship between extrusion height and width. To do this, we fitted a curve to the logarithm values of height and width and tested the statistical significance of the height–width relationship (Figure 9). We found that linear models provided a good fit to the data with the slope of the filtered dataset having a slightly higher value since the rhyolites are excluded. The p -values are significant in both instances ($p_{\text{Full}} = 1.53 \times 10^{-53}$, $p_{\text{Final}} = 1.02 \times 10^{-28}$), indicating that the two parameters are related in a statistically significant manner. We therefore conclude that the relationship between extrusion height and width follows a power-law distribution. Figure 9 also provides evidence that a truncated power law may be a more accurate description of the relationship between extrusion height and width since the extreme ends of the data field are much less populated than the central region.

We propose two explanations for the apparent truncation of the power-law relationship at lower height and width values. The first is a systematic under-sampling of smaller lava domes, since early lava dome growth often goes unobserved or unrecorded. Small extrusions may be especially vulnerable to under-sampling due to being obstructed from view, either by gas emissions and cloud cover or by crater walls surrounding the growing extrusion [Wadge et al. 2009; Diefenbach et al. 2012; Valade et al. 2019]. The second is that the physical characteristics of magmas and conduits limit the minimum size of an extrusion. Studies have demonstrated that magma discharge rates decrease as conduit diameter decreases [Melnik et al. 2005; Manga et al. 2018], and so it follows that there exists a minimum conduit diameter through which magma can flow. This could also relate to the increased resistance to buoyancy-driven ascent of magma in a narrow conduit, whereby the volume of rising magma must be sufficiently large for the buoyant force to exceed the resistant force [Lavallée et al. 2012; Caricchi et al. 2014]. Therefore, we can assume that a fresh extrusion must have a minimum possible width that is dictated by conduit geometry.

The maximum dimensions and aspect ratio that a viscous extrusion can reach and maintain may also be governed by several physical processes. We observe a maximum aspect ratio of 3.16, with the frequency of observations reducing with increasing aspect ratio or height values (Figure 2). The rarity of observations with high aspect ratios may be the result of a very specific but uncommon set of physical conditions being

required or may be due to the narrow observation window resulting from the transient, short-lived nature of these structures. The maximum height for a given aspect ratio likely relates to the strength of the extruded material [Zorn et al. 2020] and is self-limiting, with taller or higher aspect ratio structures undergoing collapse or spalling to maintain stability. Increased rates of material spalling with continued extrusion have also been observed in analogue models of lava dome growth, whereby mass transfer downslope increases the basal diameter of the extrusion [Zorn et al. 2020]. As viscous extrusions continue to grow, they undergo lateral spreading to increase the gravitational stability of the system [Hale et al. 2009; Diefenbach et al. 2013; Harnett et al. 2019]. There are also a number of parameters that exert an upper limit on the width of a viscous extrusion, including viscosity, eruption volume, and topographic confinement. Furthermore, there exists a bias in the terminology used, meaning that very wide extrusions are reclassified as coulees or flows as opposed to domes, thus reducing the frequency of records taken from the literature.

4.3 The role of magma composition in lava dome/spine geometry

We have demonstrated that lava domes and lava spines are primarily observed at volcanoes with basaltic andesite, andesite, or dacite magmas. For the filtered dataset which includes basaltic andesites, andesites, and dacites, we find no statistically significant role of composition in their geometry. Conclusions around the role of magma composition in lava dome and lava spine growth do, however, need to be made cautiously. The sample sizes of young (<250 years) basaltic, trachytic, and rhyolitic domes are small, ranging from $n_{\text{trachyte}} = 2$ to $n_{\text{rhyolite}} = 5$.

Our analysis suggests that the most significant parameter controlling whether an extrusion can form a lava dome is the effective viscosity of the extruding lava. Whilst the effective viscosity is largely controlled by the composition of the melt, it is also affected by temperature, ascent rate, crystallinity, porosity, and volatile content [Melnik et al. 2005; Cassidy et al. 2015]. Analogue modelling studies have highlighted the importance of ascent rate on resulting extrusion geometry [e.g. Fink and Bridges 1995] and provide a useful way to assess the role of each of the variables influencing extrusion geometry independently (e.g. viscosity using a plaster slurry [Závada et al. 2009]). Trying to quantify the effect of each variable in a natural system with multiple confounding parameters, however, remains a challenge.

Numerical modelling is also increasingly utilised to investigate the effect of varying parameters on extrusion geometry. Modelling of the lava dome at Volcán de Colima by Zeinalova et al. [2021] has highlighted the significance of degassing-induced crystallisation as a mechanism of increasing magma viscosity and thus promoting lava dome formation. The importance of crystallisation as a mechanism to increase viscosity is further illustrated by Villeneuve et al. [2008]. By remelting basalt samples from Piton de la Fournaise (Réunion), they demonstrated that it is possible to reach viscosities as high as 10^{12} Pa·s through crystallisation and cooling. This find-

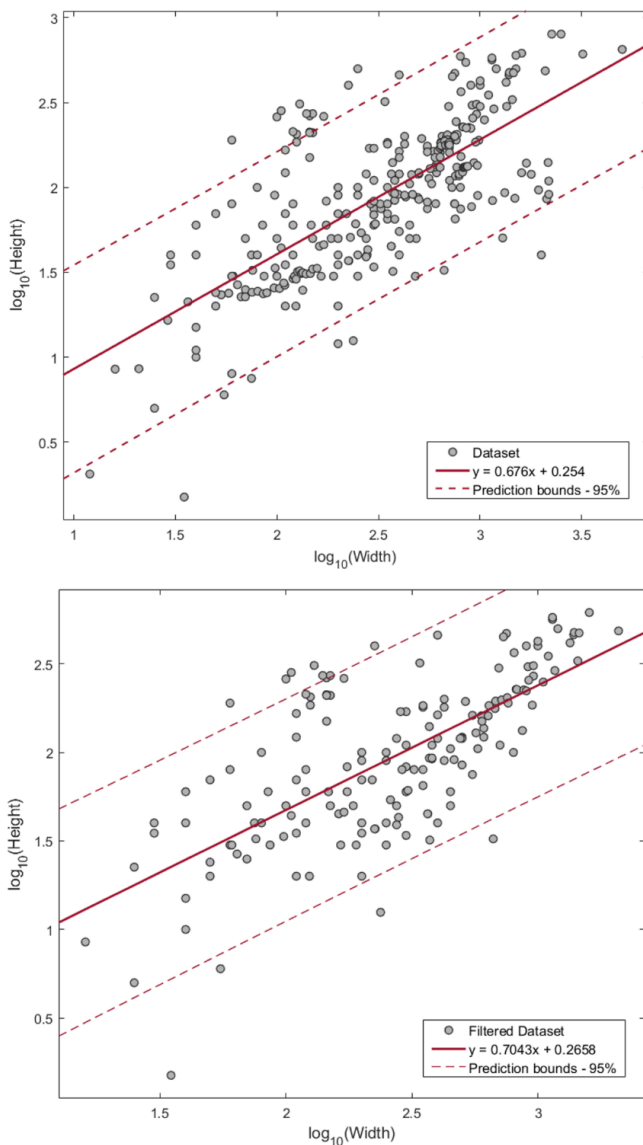


Figure 9: Modelled linear fit to the logarithmic values of height and width for the full and final filtered datasets. The linear fit has a higher slope parameter for the filtered dataset as it no longer includes low AR rhyolites. The lower density of data at the extreme ends compared to the central region of the data field is consistent with a truncated power law relationship governing extrusion geometry.

ing suggests that basaltic extrusions can have viscosities that support lava dome formation, and therefore there is a need to sample extrusions with magma compositions not traditionally associated with lava dome growth.

4.3.1 Controls on the viscosity of silicic magmas

We have presented evidence that emplacement age may influence the observed dimensions of viscous extrusions, but we acknowledge there are likely several additional factors that are difficult to test using this dataset. Many of the extrusions that plot with heights and widths away from the main trend are rhyolitic and are potentially volatile-rich compared to other magmatic compositions [Schmincke 2004]. The high volatile

content of rhyolitic magmas leads to foaming of the melt during ascent-driven exsolution, with von Aulock et al. [2017] finding that samples of obsidian glass expand by up to 400 % when heated to 950 °C. Martel and Iacono-Marziano [2015] found that, for bulk viscosities of 10^4 – 10^5 Pa·s, foamy melts begin collapsing within 24 hours at pressures <10 MPa. Foam collapse results in deflation which could lower the height and therefore the aspect ratio of the extrusion.

In addition to being volatile rich, rhyolitic magmas are often crystal poor. For example, Obsidian Dome, USA, rhyolites have crystallinities < 5 % [Swanson et al. 1989; Závada et al. 2009] whereas Bezymianny andesites have crystallinities of 35–70 % [Girina 2013]. Magmas with high crystallinities exhibit higher bulk viscosities and have higher yield strengths than their low crystallinity counterparts due to the crystals resisting flow of the melt fraction [Dragoni and Tallarico 1994; Lejeune and Richet 1995]. In a study of pre-eruptive magma viscosity, Takeuchi [2011] found that although bulk viscosities of basaltic to rhyolitic magmas ranged from 10^1 – 10^8 Pa·s, magmas classified as andesitic already span bulk viscosities on the order of 10^2 – 10^7 Pa·s depending on their crystallinities. Extrusions of a low viscosity, crystal-poor rhyolite lava may therefore have lower aspect ratios.

4.4 External controls on lava dome and lava spine geometry

Whilst the aspect ratio of a viscous extrusion often provides a good indication of the nature of the volcanic system, we suggest that it can also prove misleading without full consideration of the extrusion setting. The literature provides evidence for extrinsic controls on extrusion geometry from three main factors: (i) confinement or buttressing with a crater; (ii) extrusion onto a slope; and (iii) interaction with ice.

In the case of extrusion within a confined crater, the crater walls support the growing extrusion vertically and limit possible lateral spreading of material. This can result in a viscous extrusion with a higher aspect ratio than the equivalent material extruded onto a flat unconfined surface. Examples of lava domes growing in confined craters include Nevados de Chillán, Chile [Moussallam et al. 2021] and Popocatepetl, Mexico [Gómez-Vázquez et al. 2016]. Fourteen lava domes were extruded into a crater confined on three sides by ice and bedrock at Redoubt, USA, during the 1989–1990 eruption [Miller 1994]. Observations and monitoring of the volcano during this time revealed that the primary growth direction was vertically upwards due to confinement inhibiting lateral flow. Consequently, there were frequent dome collapses and rock-falls due to repeated oversteepening of the dome sides during vertical growth [Miller 1994].

Hale et al. [2009] demonstrate a similar process using the finite element method (FEM) to model lava dome growth at Soufrière Hills Volcano, Montserrat. Vertical growth was promoted in models where the talus slopes of the dome acted to buttress and confine the dome, thus inhibiting lateral flow. This process is observed at many dome-forming volcanoes around the globe. A dual approach using discrete element method modelling and analogue sandbox modelling was used by Walter et al. [2022] to better understand dome growth at Shiveluch, Russia. Both methods found that, for domes with

asymmetric buttresses, larger vertical displacements occur on the buttressed side of the dome. Additionally, [Walter et al. \[2022\]](#) found that the talus slope on the buttressed side sat higher than on the unbuttressed side. This behaviour is not unique to Shiveluch; equivalent observations have been made during a period of dome growth at Soufrière Hills Volcano in 2006 [[Wadge et al. 2008](#)].

Extrusion onto a slope is associated with increased lateral spread in the downslope direction due to the influence of gravity. Depending on the viewing angle when making measurements, the width of the dome could vary from a minimum along the short axis to a maximum along the long axis. The degree of additional directed spread is determined by slope angle, where steeper slopes promote increased spread. The resulting extrusion in this case has a lower aspect ratio than a simple extrusion onto a level surface, with dome thickness decreasing in the downslope direction [[Diefenbach et al. 2013](#); [Harnett and Heap 2021](#)]. [Harnett et al. \[2018\]](#) used the discrete element method to investigate lava dome emplacement under a range of conditions. They find that emplacing a dome onto a slope promotes spreading and generates wider domes compared to emplacement on a horizontal surface (the modelled dome is 212 m wide when extrusion is onto a level surface versus 232 m when extruded on a gentle slope).

A particularly well documented example of underlying slopes affecting lava dome geometry in nature is the 2009 dome growth at Redoubt [[Diefenbach et al. 2013](#)]. The lava dome was emplaced within the summit crater left after the 1989–1990 eruptive episode and eventually overtopped the crater walls. The resulting dome lies within the glacial gorge and has a teardrop geometry, whereby the downslope portion has a tapering width and extends further from the vent than the upslope portion. During the 2009 activity at Redoubt, measurements of a lava dome after overtopping the crater wall gave a height of 200 m and a width of 750 m, corresponding to an aspect ratio of 0.27. [Diefenbach et al. \[2013\]](#) analysed the height difference through time across the dome and found that, towards the end of the extrusive phase, the portion of the dome centred above the vent experienced the least vertical growth since material was being redistributed downslope. A further example is seen in the 1991–1994 growth profiles at Mount Unzen [[Nakada and Fujii 1993](#); [Nakada and Shimizu 2013](#)]. The lava dome growing in 1991 had aspect ratios of 0.42–0.50, corresponding to when growth was confined within the crater. Once the growing dome had overtopped the wall, the aspect ratio decreased and remained below 0.28 for the entire 1993–1994 period.

If dome extrusion is restarted after a pause, there may be a plug of more solid material at the top of the conduit that needs to either be forced out of the conduit or bypassed by ascending magma [[Iverson 2008](#); [Ryan et al. 2018](#); [Shevchenko et al. 2020](#)]. Likewise, the presence of ice cover can impart a directionality to dome and spine extrusion due to the different resistance imparted by ice and rock, as seen at Mount St. Helens [e.g. [Vallance et al. 2008](#)]. [Walder et al. \[2007\]](#) documented changes to the crater glacier at Mount St. Helens during the 2004–2005 dome growth period. They observed a near-solid plug rise and split the glacial ice into an eastern and western

portion before a series of spines were extruded. Growth was initially directed to the east, evidenced by the reduced aerial extent and greater thickness of the eastern arm of the glacier [[Walder et al. 2007](#)]. Each new spine grew over and forced previously extruded material and glacial ice to the side, much like a snow plough. This is evidenced by the changing aspect ratio for the different spine building phases during the 2004–2005 activity [[Vallance et al. 2008](#)]. Spine 1 extruded with aspect ratios ranging between 0.50 and 0.71. By the extrusion of Spine 3, the aspect ratio of the spine had increased to 1.03–1.78. Spine 5 extruded with aspect ratios of 1.54–2.70, likely as a result of the pre-existing domes filling a significant volume of the eastern crater. [Walder et al. \[2007\]](#) noted the glacial ice being pushed against the crater walls and thickening as successive spines were extruded, with an approximately equal degree of thickening in both the eastern and western arm. Analysis showed the extruded material was largely degassed with high crystallinity in addition to being extruded at relatively low temperatures, hence the tendency toward high aspect ratio geometries, a finding that was supported by results from laboratory deformation experiments conducted by [Heap et al. \[2016\]](#).

4.5 Temporal evolution of the height and width of lava domes and spines

For the domes with time series data that we investigated, growth broadly follows a common path through time whereby we observe initial increases in extrusion heights and widths, before the rate of increase slows and approximately constant aspect ratios are maintained. This holds true for volcanoes at a range of scales and of different compositions ([Figure 10](#)). Similar growth profiles have been observed for normalised extrusion volumes through time [[Anderson and Segall 2011](#)].

The completeness of a time series is difficult to determine without independent and detailed verification of the recent eruptive history. Capturing the very beginning of lava dome growth into a crater or event scar after a previous complete dome collapse event will yield a time series starting at very low height and width. If, on the other hand, dome growth is continuing after a pause in activity, then the time series record will start with a pre-established dome geometry. Interpreting the time series datasets presented in this paper comes with similar difficulties. The dataset from Volcán de Colima appears consistent with growth of a fresh dome, and this is verified by the optical imagery from [Walter et al. \[2019\]](#). The dataset from Mount Unzen, on the other hand, begins with a dome with height and width of 132 and 630 m respectively [[Nakada and Shimizu 2013](#)]. This could either be the result of the onset of dome growth being missed or restarting extrusion after a pause. With the improvements in technology, it is hoped that, in future, more detailed and consistent monitoring of lava domes from the onset of growth will facilitate our understanding of dome growth patterns and potential hazards at different stages.

4.6 Probabilistic hazard assessment

We have shown that the Weibull distribution model provides a good approximation to height, width, and aspect ratio data

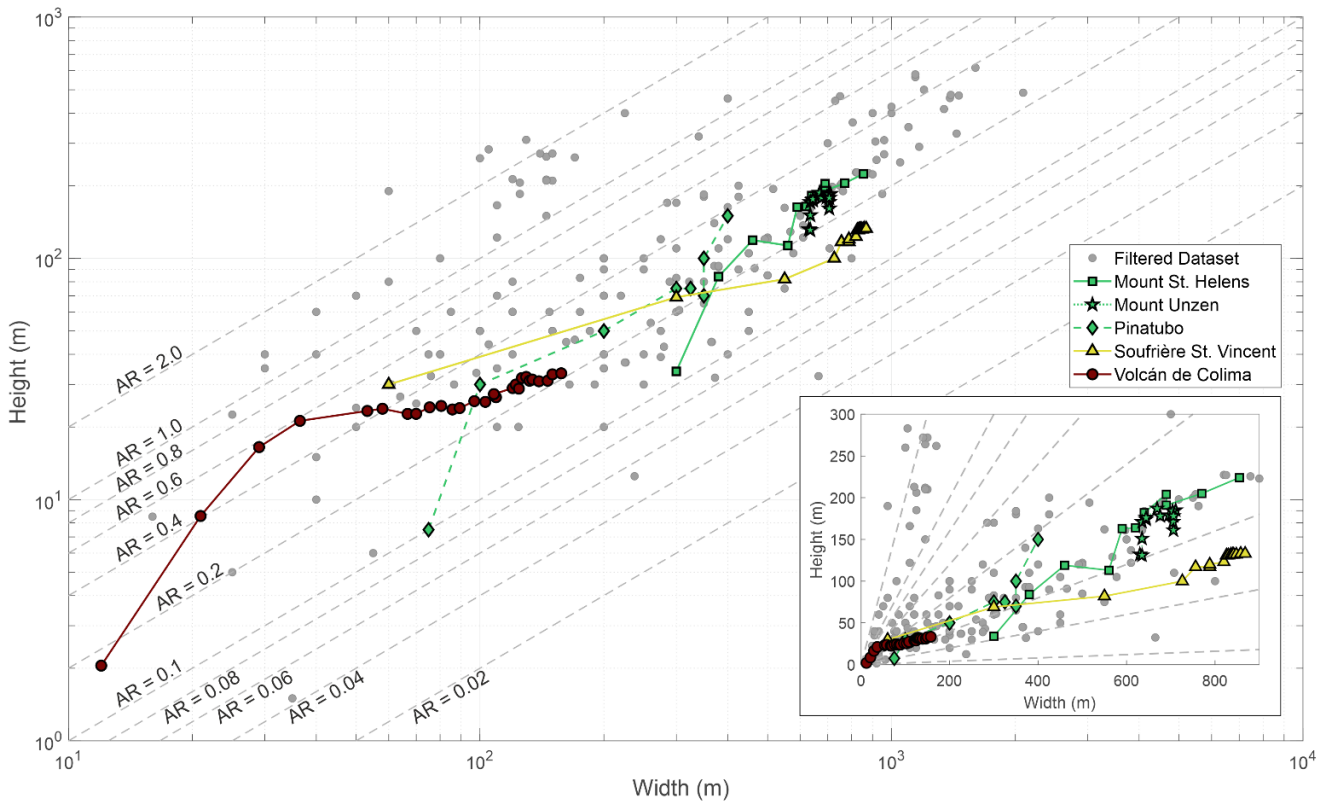


Figure 10: Growth evolution curves of the time series records contained in the dataset, overlaying point measurement data. Inset figure shows the curves on linear axes to better represent the relative spatial scales of the different extrusions.

describing viscous extrusions, and we suggest that this can be used to assist in probabilistic hazard forecasting. Probabilistic forecasting incorporates observed current activity with knowledge of past events to estimate the likelihood of future events over timescales of hours to weeks [Connor et al. 2015; McNutt et al. 2015]. Wadge et al. [2009] highlighted the influence of lava dome height on the collapse direction for a given topography at Soufrière Hills Volcano; knowing the distribution of extrusion heights found in nature can therefore constrain the probability of an extrusion reaching a given height and guide the input values used in forecast models. Our lava dome dimension dataset can further be used to approximate dome volume calculations, which are crucial for pyroclastic density current forecast modelling [Cole et al. 2015; Neri et al. 2015]. Access to multiple high-quality comprehensive datasets is therefore crucial to both informing input parameters and guiding probabilities given in volcanic event trees [Marzocchi and Bebbington 2012; Newhall and Pallister 2015; Wolpert et al. 2016; Papale 2021]. Such global datasets allow forecasters to account for a full range of possible scenarios, thus complementing localised event histories for individual volcanoes.

5 CONCLUSIONS

In this study, we have collated 323 measurements concerning the heights and widths of viscous extrusions to generate a global dataset recording Morphology of Viscous Extrusions (MoVE). Sources included but were not limited to journal articles, observatory reports, and activity bulletins. We carried out a statistical analysis into the distributions of height, width,

and aspect ratio, the relationship between these parameters, and the role of composition in extrusion geometry. From the results of this analysis on the compiled dataset, we conclude the following:

- (1) Height and width data do not follow a normal distribution, but instead exhibit a strong positive skew. A two-parameter Weibull distribution provides a good fit to the data, suggesting the dataset is lacking measurements from very small extrusions.
- (2) The age of the extrusion plays a role in extrusion geometry, with the aspect ratio of older extrusions shifted to lower values.
- (3) We find no statistically significant effect of magma composition on the recorded heights and widths of viscous extrusions for the filtered dataset that includes basaltic andesite, andesite, and dacite compositional groups. Due to the age filtering and low statistical reliability of groups with small sample sizes, data from the basalt, trachyte, and rhyolite compositional groups were excluded from analysis. To gain a more thorough understanding of the role magma composition plays on extrusion geometry, a larger and more complete dataset is required.
- (4) The dataset yields probability density functions that can provide the basis for forecasting future hazard footprints related to extrusion geometry, such as approximating lava dome volumes and identifying the most likely dome collapse direction(s).

The dataset used in this study is freely available and we encourage members of the volcanology community to use and contribute to this resource. Time series datasets provide an important means of identifying different growth paths of lava extrusions, and we suggest datasets with improved sampling rates can aid identification of the typical lava dome growth paths, which can feed into hazard assessment during active eruptions. Lastly, increasing the frequency with which properties such as extrusion volume are recorded will provide additional opportunities to investigate what influences extrusion geometry in a statistically robust manner.

AUTHOR CONTRIBUTIONS

AM: Conceptualization, Data Curation, Formal Analysis, Investigation, Visualization, Writing – original draft; CH: Conceptualization, Funding acquisition, Investigation, Supervision, Writing – review and editing; EH: Conceptualization, Investigation, Supervision, Writing – review and editing; TW: Supervision, Writing – review and editing; MH: Supervision, Writing – review and editing.

ACKNOWLEDGEMENTS

This type of database would not be possible without daily efforts from observatory staff. We thank Sarah Ogburn for sharing data and invaluable discussion on the data analysis and manuscript. We also thank Karim Kelfoun for provision of additional data. AM was funded through an Ad Astra Scholarship from University College Dublin. AM and CH acknowledge support from a Royal Irish Academy Charlemont Grant. CH acknowledges support from the Ambassade de France en Irlande Excellence Research Residency. MH and CH acknowledge support from a Ulysses Grant (Grant Number 47199ZM) implemented by the Ministry for Europe and Foreign Affairs (MEAE) and the Ministry of Higher Education and Research (MESR) in France and by the Irish Research Council (IRC) in Ireland. MH acknowledges support from the Institut Universitaire de France (IUF). We acknowledge the thorough, detailed and constructive reviews from three reviewers which helped improve this manuscript.

DATA AVAILABILITY

The full MoVE dataset, with relevant references, is available open access on Vhub: <https://thehub.org/resources/4988>.

COPYRIGHT NOTICE

© The Author(s) 2024. This article is distributed under the terms of the [Creative Commons Attribution 4.0 International License](https://creativecommons.org/licenses/by/4.0/), which permits unrestricted use, distribution, and reproduction in any medium, provided you give appropriate credit to the original author(s) and the source, provide a link to the Creative Commons license, and indicate if changes were made.

REFERENCES

- Anderson, K. and P. Segall (2011). “Physics-based models of ground deformation and extrusion rate at effusively erupting volcanoes”. *Journal of Geophysical Research* 116(B7). DOI: [10.1029/2010jb007939](https://doi.org/10.1029/2010jb007939).
- Ashwell, P. A., B. M. Kennedy, M. Edwards, and J. W. Cole (2018). “Characteristics and consequences of lava dome collapse at Ruawahia, Taupo Volcanic Zone, New Zealand”. *Bulletin of Volcanology* 80(5). DOI: [10.1007/s00445-018-1217-1](https://doi.org/10.1007/s00445-018-1217-1).
- Blake, S. (1990). “Viscoplastic Models of Lava Domes”. *Lava Flows and Domes*. Edited by J. H. Fink. Springer Berlin Heidelberg, pages 88–126. ISBN: 9783642743795. DOI: [10.1007/978-3-642-74379-5_5](https://doi.org/10.1007/978-3-642-74379-5_5).
- Blower, J., J. Keating, H. Mader, and J. Phillips (2003). “The evolution of bubble size distributions in volcanic eruptions”. *Journal of Volcanology and Geothermal Research* 120(1–2), pages 1–23. DOI: [10.1016/S0377-0273\(02\)00404-3](https://doi.org/10.1016/S0377-0273(02)00404-3).
- Calder, E. S., Y. Lavallée, J. E. Kendrick, and M. Bernstein (2015). “Lava Dome Eruptions”. *The Encyclopedia of Volcanoes*. Edited by H. Sigurdsson, B. Houghton, S. R. McNutt, H. Rymer, and J. Stix. 2nd edition. Elsevier, pages 343–362. ISBN: 9780123859389. DOI: [10.1016/c2015-0-00175-7](https://doi.org/10.1016/c2015-0-00175-7).
- Caricchi, L., C. Annen, J. Blundy, G. Simpson, and V. Pinel (2014). “Frequency and magnitude of volcanic eruptions controlled by magma injection and buoyancy”. *Nature Geoscience* 7, pages 126–130. DOI: [10.1038/ngeo2041](https://doi.org/10.1038/ngeo2041).
- Carr, B. B., E. Lev, L. Vanderkluyzen, D. Moyer, G. I. Marliyani, and A. B. Clarke (2022). “The Stability and Collapse of Lava Domes: Insight From Photogrammetry and Slope Stability Models Applied to Sinabung Volcano (Indonesia)”. *Frontiers in Earth Science* 10. DOI: [10.3389/feart.2022.813813](https://doi.org/10.3389/feart.2022.813813).
- Cassidy, M., P. Cole, K. E. Hicks, N. R. Varley, N. Peters, and A. H. Lerner (2015). “Rapid and slow: Varying magma ascent rates as a mechanism for Vulcanian explosions”. *Earth and Planetary Science Letters* 420, pages 73–84. DOI: [10.1016/j.epsl.2015.03.025](https://doi.org/10.1016/j.epsl.2015.03.025).
- Cole, P. D., A. Neri, and P. J. Baxter (2015). “Hazards from Pyroclastic Density Currents”. *The Encyclopedia of Volcanoes*. Elsevier, pages 943–956. ISBN: 9780123859389. DOI: [10.1016/b978-0-12-385938-9.00054-7](https://doi.org/10.1016/b978-0-12-385938-9.00054-7).
- Connor, C., M. Bebbington, and W. Marzocchi (2015). “Probabilistic Volcanic Hazard Assessment”. *The Encyclopedia of Volcanoes*. Elsevier, pages 897–910. ISBN: 9780123859389. DOI: [10.1016/b978-0-12-385938-9.00051-1](https://doi.org/10.1016/b978-0-12-385938-9.00051-1).
- Coombs, M., K. Bull, C. Nye, D. Schneider, J. Vallance, and R. Wessels (2010). “Timing, distribution, and volume of proximal products of the 2006 eruption of Augustine Volcano”. *The 2006 eruption of Augustine Volcano, Alaska: U.S. Geological Survey Professional Paper 1769*. Edited by J. A. Power, M. L. Coombs, and J. T. Freymueller. U.S. Geological Survey, pages 145–186. DOI: [10.3133/pp17698](https://doi.org/10.3133/pp17698).
- Corral, Á. and Á. González (2019). “Power Law Size Distributions in Geoscience Revisited”. *Earth and Space Science* 6(5), pages 673–697. DOI: [10.1029/2018ea000479](https://doi.org/10.1029/2018ea000479).

- Daag, A. S., M. T. Dolan, E. P. Laguerta, G. P. Meeker, C. G. Newhall, J. S. Pallister, and R. U. Solidum (1996). "Growth of a Postclimactic Lava Dome at Mount Pinatubo, July–October 1992". *Fire and Mud: Eruptions and Lahars of Mount Pinatubo, Philippines*. Edited by C. G. Newhall and R. S. Punongbayan. Philippine Institute of Volcanology, Seismology, Quezon City; University of Washington Press, Seattle, and London. ISBN: 0295975857.
- Daggitt, M. L., T. A. Mather, D. M. Pyle, and S. Page (2014). "AshCalc—a new tool for the comparison of the exponential, power-law and Weibull models of tephra deposition". *Journal of Applied Volcanology* 3(1). DOI: [10.1186/2191-5040-3-7](https://doi.org/10.1186/2191-5040-3-7).
- Diefenbach, A. K., K. F. Bull, R. L. Wessels, and R. G. McGimsey (2013). "Photogrammetric monitoring of lava dome growth during the 2009 eruption of Redoubt Volcano". *Journal of Volcanology and Geothermal Research* 259, pages 308–316. DOI: [10.1016/j.jvolgeores.2011.12.009](https://doi.org/10.1016/j.jvolgeores.2011.12.009).
- Diefenbach, A. K., J. G. Crider, S. P. Schilling, and D. Dzurisin (2012). "Rapid, low-cost photogrammetry to monitor volcanic eruptions: an example from Mount St. Helens, Washington, USA". *Bulletin of Volcanology* 74(2), pages 579–587. DOI: [10.1007/s00445-011-0548-y](https://doi.org/10.1007/s00445-011-0548-y).
- Dragoni, M. and A. Tallarico (1994). "The effect of crystallization on the rheology and dynamics of lava flows". *Journal of Volcanology and Geothermal Research* 59(3), pages 241–252. DOI: [10.1016/0377-0273\(94\)90098-1](https://doi.org/10.1016/0377-0273(94)90098-1).
- Duffield, W. A. and C. R. Bacon (1981). *Geologic map of the Coso volcanic field and adjacent areas, Inyo County, California*. Volume IMAP. 1200. U.S. Geological Survey. DOI: [10.3133/i1200](https://doi.org/10.3133/i1200). [scale 1:50,000].
- Fink, J. H. and N. T. Bridges (1995). "Effects of eruption history and cooling rate on lava dome growth". *Bulletin of Volcanology* 57(4), pages 229–239. DOI: [10.1007/bf00265423](https://doi.org/10.1007/bf00265423).
- Fink, J. H. and R. W. Griffiths (1998). "Morphology, eruption rates, and rheology of lava domes: Insights from laboratory models". *Journal of Geophysical Research: Solid Earth* 103(B1), pages 527–545. DOI: [10.1029/97jb02838](https://doi.org/10.1029/97jb02838).
- Giordano, D., J. K. Russell, and D. B. Dingwell (2008). "Viscosity of magmatic liquids: A model". *Earth and Planetary Science Letters* 271(1–4), pages 123–134. DOI: [10.1016/j.epsl.2008.03.038](https://doi.org/10.1016/j.epsl.2008.03.038).
- Girina, O. A. (2013). "Chronology of Bezymianny Volcano activity, 1956–2010". *Journal of Volcanology and Geothermal Research* 263, pages 22–41. DOI: [10.1016/j.jvolgeores.2013.05.002](https://doi.org/10.1016/j.jvolgeores.2013.05.002).
- Glen, S. (2023). *Power Law and Power Law Distribution*. URL: <https://www.statisticshowto.com/power-law/> (visited on 08/30/2024).
- Global Volcanism Program (GVP) (2023). *Volcanoes of the World, v.5.1.0*. Edited by E. Venzke. Global Volcanism Program. DOI: [10.5479/si.gvp.votw5-2023.5.1](https://doi.org/10.5479/si.gvp.votw5-2023.5.1).
- Gómez-Vazquez, A., S. De la Cruz-Reyna, and A. T. Mendoza-Rosas (2016). "The ongoing dome emplacement and destruction cyclic process at Popocatepetl volcano, Central Mexico". *Bulletin of Volcanology* 78(9). DOI: [10.1007/s00445-016-1054-z](https://doi.org/10.1007/s00445-016-1054-z).
- Green, J. and N. M. Short (1971). *Volcanic Landforms and Surface Features: A Photographic Atlas and Glossary*. Springer Berlin Heidelberg. ISBN: 9783642651502. DOI: [10.1007/978-3-642-65150-2](https://doi.org/10.1007/978-3-642-65150-2).
- Griffiths, R. W. (2000). "The Dynamics of Lava Flows". *Annual Review of Fluid Mechanics* 32(1), pages 477–518. DOI: [10.1146/annurev.fluid.32.1.477](https://doi.org/10.1146/annurev.fluid.32.1.477).
- Hale, A., E. Calder, S. Loughlin, G. Wadge, and G. Ryan (2009). "Modelling the lava dome extruded at Soufrière Hills Volcano, Montserrat, August 2005–May 2006". *Journal of Volcanology and Geothermal Research* 187(1–2), pages 69–84. DOI: [10.1016/j.jvolgeores.2009.08.014](https://doi.org/10.1016/j.jvolgeores.2009.08.014).
- Harnett, C. E. and M. J. Heap (2021). "Mechanical and topographic factors influencing lava dome growth and collapse". *Journal of Volcanology and Geothermal Research* 420, page 107398. DOI: [10.1016/j.jvolgeores.2021.107398](https://doi.org/10.1016/j.jvolgeores.2021.107398).
- Harnett, C. E., M. E. Thomas, E. S. Calder, S. K. Ebmeier, A. Telford, W. Murphy, and J. Neuberg (2019). "Presentation and analysis of a worldwide database for lava dome collapse events: the Global Archive of Dome Instabilities (GLADIS)". *Bulletin of Volcanology* 81(3). DOI: [10.1007/s00445-019-1276-y](https://doi.org/10.1007/s00445-019-1276-y).
- Harnett, C. E., M. E. Thomas, M. D. Purvance, and J. Neuberg (2018). "Using a discrete element approach to model lava dome emplacement and collapse". *Journal of Volcanology and Geothermal Research* 359, pages 68–77. DOI: [10.1016/j.jvolgeores.2018.06.017](https://doi.org/10.1016/j.jvolgeores.2018.06.017).
- Heap, M. J., C. E. Harnett, T. Nazarbajov, Z. Heng, P. Baud, T. Xu, M. Rosas-Carbajal, and J.-C. Komorowski (2023). "The influence of heterogeneity on the strength of volcanic rocks and the stability of lava domes". *Bulletin of Volcanology* 85(9). DOI: [10.1007/s00445-023-01669-6](https://doi.org/10.1007/s00445-023-01669-6).
- Heap, M. J., J. K. Russell, and L. A. Kennedy (2016). "Mechanical behaviour of dacite from Mount St. Helens (USA): A link between porosity and lava dome extrusion mechanism (dome or spine)?" *Journal of Volcanology and Geothermal Research* 328, pages 159–177. DOI: [10.1016/j.jvolgeores.2016.10.015](https://doi.org/10.1016/j.jvolgeores.2016.10.015).
- Huppert, H. E., J. B. Shepherd, R. Haraldur Sigurdsson, and S. J. Sparks (1982). "On lava dome growth, with application to the 1979 lava extrusion of the soufrière of St. Vincent". *Journal of Volcanology and Geothermal Research* 14(3–4), pages 199–222. DOI: [10.1016/0377-0273\(82\)90062-2](https://doi.org/10.1016/0377-0273(82)90062-2).
- Hutchison, W., N. Varley, D. M. Pyle, T. A. Mather, and J. A. Stevenson (2013). "Airborne thermal remote sensing of the Volcán de Colima (Mexico) lava dome from 2007 to 2010". *Geological Society, London, Special Publications* 380(1), pages 203–228. DOI: [10.1144/sp380.8](https://doi.org/10.1144/sp380.8).
- Iverson, R. M. (2008). "Dynamics of seismogenic volcanic extrusion resisted by a solid surface plug, Mount St. Helens, 2004–2005". *A volcano rekindled: the renewed eruption of Mount St. Helens, 2004–2006: U.S. Geological Survey Professional Paper 1750*. Edited by D. R. Sherrod, W. E. Scott, and P. H. Stauffer, pages 425–460. DOI: [10.3133/pp175021](https://doi.org/10.3133/pp175021).

- Kelfoun, K., A. B. Santoso, T. Latchimy, M. Bontemps, I. Nurdien, F. Beauducel, A. Fahmi, R. Putra, N. Dahamna, A. Laurin, M. H. Rizal, J. T. Sukmana, and V. Gueugneau (2021). “Growth and collapse of the 2018–2019 lava dome of Merapi volcano”. *Bulletin of Volcanology* 83(2). DOI: [10.1007/s00445-020-01428-x](https://doi.org/10.1007/s00445-020-01428-x).
- Krumbholz, M., C. F. Hieronymus, S. Burchardt, V. R. Troll, D. C. Tanner, and N. Friese (2014). “Weibull-distributed dyke thickness reflects probabilistic character of host-rock strength”. *Nature Communications* 5(1). DOI: [10.1038/ncomms4272](https://doi.org/10.1038/ncomms4272).
- Lacroix, A. (1904). *La Montagne Pelée et ses éruptions*. Volume 1. Masson Paris.
- Lavallée, Y., N. R. Varley, M. A. Alatorre-Ibargüengoitia, K.-U. Hess, U. Kueppers, S. Mueller, D. Richard, B. Scheu, O. Spieler, and D. B. Dingwell (2012). “Magmatic architecture of dome-building eruptions at Volcán de Colima, Mexico”. *Bulletin of Volcanology* 74(1), pages 249–260. DOI: [10.1007/s00445-011-0518-4](https://doi.org/10.1007/s00445-011-0518-4).
- Lejeune, A.-M. and P. Richet (1995). “Rheology of crystal-bearing silicate melts: An experimental study at high viscosities”. *Journal of Geophysical Research: Solid Earth* 100(B3), pages 4215–4229. DOI: [10.1029/94jb02985](https://doi.org/10.1029/94jb02985).
- Major, J., D. Dzurisin, S. Schilling, and M. Poland (2009). “Monitoring lava-dome growth during the 2004–2008 Mount St. Helens, Washington, eruption using oblique terrestrial photography”. *Earth and Planetary Science Letters* 286(1–2), pages 243–254. DOI: [10.1016/j.epsl.2009.06.034](https://doi.org/10.1016/j.epsl.2009.06.034).
- Manga, M., S. J. Mitchell, W. Degruyter, and R. J. Carey (2018). “Transition of eruptive style: Pumice raft to dome-forming eruption at the Havre submarine volcano, southwest Pacific Ocean”. *Geology* 46(12), pages 1075–1078. DOI: [10.1130/g45436.1](https://doi.org/10.1130/g45436.1).
- Martel, C. and G. Iacono-Marziano (2015). “Timescales of bubble coalescence, outgassing, and foam collapse in decompressed rhyolitic melts”. *Earth and Planetary Science Letters* 412, pages 173–185. DOI: [10.1016/j.epsl.2014.12.010](https://doi.org/10.1016/j.epsl.2014.12.010).
- Marzocchi, W. and M. S. Bebbington (2012). “Probabilistic eruption forecasting at short and long time scales”. *Bulletin of Volcanology* 74(8), pages 1777–1805. DOI: [10.1007/s00445-012-0633-x](https://doi.org/10.1007/s00445-012-0633-x).
- McNutt, S. R., G. Thompson, J. Johnson, S. D. Angelis, and D. Fee (2015). “Seismic and Infrasonic Monitoring”. *The Encyclopedia of Volcanoes*. Elsevier, pages 1071–1099. ISBN: 9780123859389. DOI: [10.1016/b978-0-12-385938-9.00063-8](https://doi.org/10.1016/b978-0-12-385938-9.00063-8).
- Melnik, O., A. Barmin, and R. Sparks (2005). “Dynamics of magma flow inside volcanic conduits with bubble overpressure buildup and gas loss through permeable magma”. *Journal of Volcanology and Geothermal Research* 143(1–3), pages 53–68. DOI: [10.1016/j.jvolgeores.2004.09.010](https://doi.org/10.1016/j.jvolgeores.2004.09.010).
- Miller, T. P. (1994). “Dome growth and destruction during the 1989–1990 eruption of redoubt volcano”. *Journal of Volcanology and Geothermal Research* 62(1–4), pages 197–212. DOI: [10.1016/0377-0273\(94\)90034-5](https://doi.org/10.1016/0377-0273(94)90034-5).
- Moussallam, Y., T. Barnie, Á. Amigo, K. Kelfoun, F. Flores, L. Franco, C. Cardona, L. Cordova, and V. Toloza (2021). “Monitoring and forecasting hazards from a slow growing lava dome using aerial imagery, tri-stereo Pleiades-1A/B imagery and PDC numerical simulation”. *Earth and Planetary Science Letters* 564, page 116906. DOI: [10.1016/j.epsl.2021.116906](https://doi.org/10.1016/j.epsl.2021.116906).
- Nakada, S. and H. Shimizu (2013). “Unzendake”. *National Catalogue of the Active Volcanoes in Japan*. 4th edition. Japan Meteorological Agency.
- Nakada, S. and T. Fujii (1993). “Preliminary report on the activity at Unzen Volcano (Japan), November 1990–November 1991: Dacite lava domes and pyroclastic flows”. *Journal of Volcanology and Geothermal Research* 54(3–4), pages 319–333. DOI: [10.1016/0377-0273\(93\)90070-8](https://doi.org/10.1016/0377-0273(93)90070-8).
- Neri, A., T. Esposti Ongaro, B. Voight, and C. Widiwijayanti (2015). “Pyroclastic Density Current Hazards and Risk”. *Volcanic Hazards, Risks and Disasters*. Edited by J. F. Shroder and P. Papale. Elsevier, pages 109–140. ISBN: 9780123964533. DOI: [10.1016/b978-0-12-396453-3.00005-8](https://doi.org/10.1016/b978-0-12-396453-3.00005-8).
- Newhall, C. G., A. S. Daag, F. G. Delfin Jr., R. P. Hoblitt, J. McGeehin, J. S. Pallister, M. T. M. Regalado, M. Rubin, B. S. Tubianosa, R. A. Tamayo Jr., and J. V. Umbal (1996). “Eruptive History of Mount Pinatubo”. *Fire and Mud: Eruptions and Lahars of Mount Pinatubo, Philippines*. Edited by C. G. Newhall and R. S. Punongbayan. Philippine Institute of Volcanology, Seismology, Quezon City; University of Washington Press, Seattle, and London. ISBN: 0295975857.
- Newhall, C. G. and J. S. Pallister (2015). “Using Multiple Data Sets to Populate Probabilistic Volcanic Event Trees”. *Volcanic Hazards, Risks and Disasters*. Elsevier, pages 203–232. ISBN: 9780123964533. DOI: [10.1016/b978-0-12-396453-3.00008-3](https://doi.org/10.1016/b978-0-12-396453-3.00008-3).
- Ogburn, S. E., S. C. Loughlin, and E. S. Calder (2012). *Dome-Haz - Dome Forming Eruptions*. URL: <https://thegithub.org/resources/1742>.
- (2015). “The association of lava dome growth with major explosive activity (VEI \geq 4): DomeHaz, a global dataset”. *Bulletin of Volcanology* 77(5). DOI: [10.1007/s00445-015-0919-x](https://doi.org/10.1007/s00445-015-0919-x).
- Ordoñez, M., C. Laverde, and M. Battaglia (2022). “The new lava dome growth of Nevado del Ruiz (2015–2021)”. *Journal of Volcanology and Geothermal Research* 430, page 107626. DOI: [10.1016/j.jvolgeores.2022.107626](https://doi.org/10.1016/j.jvolgeores.2022.107626).
- Papale, P. (2021). “Some relevant issues in volcanic hazard forecasts and management of volcanic crisis”. *Forecasting and Planning for Volcanic Hazards, Risks, and Disasters*. Elsevier, pages 1–24. ISBN: 9780128180822. DOI: [10.1016/b978-0-12-818082-2.00001-9](https://doi.org/10.1016/b978-0-12-818082-2.00001-9).
- Rhodes, E., B. M. Kennedy, Y. Lavallée, A. Hornby, M. Edwards, and G. Chigna (2018). “Textural Insights Into the Evolving Lava Dome Cycles at Santiaguito Lava Dome, Guatemala”. *Frontiers in Earth Science* 6. DOI: [10.3389/feart.2018.00030](https://doi.org/10.3389/feart.2018.00030).
- Roche, O., N. Azzaoui, and A. Guillin (2021). “Discharge rate of explosive volcanic eruption controls runout distance of pyroclastic density currents”. *Earth and Planetary Science Letters* 568, page 117017. DOI: [10.1016/j.epsl.2021.117017](https://doi.org/10.1016/j.epsl.2021.117017).

- Rogers, N. (2015). “The Composition and Origin of Magmas”. *The Encyclopedia of Volcanoes*. Elsevier, pages 93–112. ISBN: 9780123859389. DOI: [10.1016/b978-0-12-385938-9.00004-3](https://doi.org/10.1016/b978-0-12-385938-9.00004-3).
- Rutherford, M. J. (2008). “Magma Ascent Rates”. *Reviews in Mineralogy and Geochemistry* 69(1), pages 241–271. DOI: [10.2138/rmg.2008.69.7](https://doi.org/10.2138/rmg.2008.69.7).
- Ryan, A. G., E. A. Friedlander, J. K. Russell, M. J. Heap, and L. A. Kennedy (2018). “Hot pressing in conduit faults during lava dome extrusion: Insights from Mount St. Helens 2004–2008”. *Earth and Planetary Science Letters* 482, pages 171–180. DOI: [10.1016/j.epsl.2017.11.010](https://doi.org/10.1016/j.epsl.2017.11.010).
- Savov, I. P., J. F. Luhr, and C. Navarro-Ochoa (2008). “Petrology and geochemistry of lava and ash erupted from Volcán Colima, Mexico, during 1998–2005”. *Journal of Volcanology and Geothermal Research* 174(4), pages 241–256. DOI: [10.1016/j.jvolgeores.2008.02.007](https://doi.org/10.1016/j.jvolgeores.2008.02.007).
- Schilling, S. P., R. A. Thompson, J. A. Messerich, and E. Y. Iwatsubo (2008). “Use of digital aerophotogrammetry to determine rates of lava dome growth, Mount St. Helens, Washington, 2004–2005”. *A volcano rekindled: the renewed eruption of Mount St. Helens, 2004–2006: U.S. Geological Survey Professional Paper 1750*. Edited by D. R. Sherrod, W. E. Scott, and P. H. Stauffer, pages 145–167. DOI: [10.3133/pp17508](https://doi.org/10.3133/pp17508).
- Schmincke, H.-U. (2004). “Rheology, Magmatic Gases, Bubbles and Triggering of Eruptions”. *Volcanism*. Springer Berlin Heidelberg, pages 35–58. ISBN: 9783642189524. DOI: [10.1007/978-3-642-18952-4_4](https://doi.org/10.1007/978-3-642-18952-4_4).
- Shevchenko, A. V., V. N. Dvigalo, T. R. Walter, R. Mania, F. Maccaferri, I. Y. Svirid, A. B. Belousov, and M. G. Belousova (2020). “The rebirth and evolution of Bezymianny volcano, Kamchatka after the 1956 sector collapse”. *Communications Earth & Environment* 1(1). DOI: [10.1038/s43247-020-00014-5](https://doi.org/10.1038/s43247-020-00014-5).
- Sparks, R. S. J. (1997). “Causes and consequences of pressurisation in lava dome eruptions”. *Earth and Planetary Science Letters* 150(3–4), pages 177–189. DOI: [10.1016/s0012-821x\(97\)00109-x](https://doi.org/10.1016/s0012-821x(97)00109-x).
- Sparks, R. S. J., M. D. Murphy, A. M. Lejeune, R. B. Watts, J. Barclay, and S. R. Young (2000). “Control on the emplacement of the andesite lava dome of the Soufriere Hills volcano, Montserrat by degassing-induced crystallization”. *Terra Nova* 12(1), pages 14–20. DOI: [10.1046/j.1365-3121.2000.00267.x](https://doi.org/10.1046/j.1365-3121.2000.00267.x).
- Swanson, D. A., D. Dzurisin, R. T. Holcomb, E. Y. Iwatsubo, W. W. Chadwick, T. J. Casadevall, J. W. Ewert, and C. C. Heliker (1987). “Growth of the lava dome at Mount St. Helens, Washington, (USA), 1981–1983”. *The Emplacement of Silicic Domes and Lava Flows*. Geological Society of America, pages 1–16. ISBN: 9780813722122. DOI: [10.1130/spe212-p1](https://doi.org/10.1130/spe212-p1).
- Swanson, D. A. and R. T. Holcomb (1990). “Regularities in Growth of the Mount St. Helens Dacite Dome, 1980–1986”. *Lava Flows and Domes*. Edited by J. H. Fink. Springer Berlin Heidelberg, pages 3–24. ISBN: 9783642743795. DOI: [10.1007/978-3-642-74379-5_1](https://doi.org/10.1007/978-3-642-74379-5_1).
- Swanson, S. E., M. T. Naney, H. R. Westrich, and J. C. Eichelberger (1989). “Crystallization history of Obsidian Dome, Inyo Domes, California”. *Bulletin of Volcanology* 51(3), pages 161–176. DOI: [10.1007/bf01067953](https://doi.org/10.1007/bf01067953).
- Takeuchi, S. (2011). “Preeruptive magma viscosity: An important measure of magma eruptibility”. *Journal of Geophysical Research* 116(B10). DOI: [10.1029/2011jb008243](https://doi.org/10.1029/2011jb008243).
- Thiele, S. T., N. Varley, and M. R. James (2017). “Thermal photogrammetric imaging: A new technique for monitoring dome eruptions”. *Journal of Volcanology and Geothermal Research* 337, pages 140–145. DOI: [10.1016/j.jvolgeores.2017.03.022](https://doi.org/10.1016/j.jvolgeores.2017.03.022).
- Valade, S., A. Ley, F. Massimetti, O. D’Hondt, M. Laiolo, D. Coppola, D. Loibl, O. Hellwich, and T. R. Walter (2019). “Towards Global Volcano Monitoring Using Multisensor Sentinel Missions and Artificial Intelligence: The MOUNTS Monitoring System”. *Remote Sensing* 11(13), page 1528. DOI: [10.3390/rs11131528](https://doi.org/10.3390/rs11131528).
- Vallance, J. W., D. J. Schneider, and S. P. Schilling (2008). “Growth of the 2004–2006 lava-dome complex at Mount St. Helens, Washington”. *A volcano rekindled: the renewed eruption of Mount St. Helens, 2004–2006: U.S. Geological Survey Professional Paper 1750*. Edited by D. R. Sherrod, W. E. Scott, and P. H. Stauffer, pages 169–208. DOI: [10.3133/pp17509](https://doi.org/10.3133/pp17509).
- Vallejo, S., A. K. Diefenbach, H. E. Gaunt, M. Almeida, P. Ramón, F. Naranjo, and K. Kelfoun (2024). “Twenty years of explosive-effusive activity at El Reventador volcano (Ecuador) recorded in its geomorphology”. *Frontiers in Earth Science* 11. DOI: [10.3389/feart.2023.1202285](https://doi.org/10.3389/feart.2023.1202285).
- Villeneuve, N., D. R. Neuville, P. Boivin, P. Bachèlery, and P. Richet (2008). “Magma crystallization and viscosity: A study of molten basalts from the Piton de la Fournaise volcano (La Réunion island)”. *Chemical Geology* 256(3–4), pages 242–251. DOI: [10.1016/j.chemgeo.2008.06.039](https://doi.org/10.1016/j.chemgeo.2008.06.039).
- Voight, B. and D. Elsworth (2000). “Instability and collapse of hazardous gas-pressurized lava domes”. *Geophysical Research Letters* 27(1), pages 1–4. DOI: [10.1029/1999gl008389](https://doi.org/10.1029/1999gl008389).
- Von Aulock, F. W., B. M. Kennedy, A. Maksimenko, F. B. Wadsworth, and Y. Lavallée (2017). “Outgassing from Open and Closed Magma Foams”. *Frontiers in Earth Science* 5. DOI: [10.3389/feart.2017.00046](https://doi.org/10.3389/feart.2017.00046).
- Wadge, G., D. G. Macfarlane, H. M. Odbert, M. R. James, J. K. Hole, G. Ryan, V. Bass, S. De Angelis, H. Pinkerton, D. A. Robertson, and S. C. Loughlin (2008). “Lava dome growth and mass wasting measured by a time series of ground-based radar and seismicity observations”. *Journal of Geophysical Research: Solid Earth* 113(B8). DOI: [10.1029/2007jb005466](https://doi.org/10.1029/2007jb005466).
- Wadge, G., G. Ryan, and E. S. Calder (2009). “Clastic and core lava components of a silicic lava dome”. *Geology* 37(6), pages 551–554. DOI: [10.1130/g25747a.1](https://doi.org/10.1130/g25747a.1).
- Walder, J. S., R. G. LaHusen, J. W. Vallance, and S. P. Schilling (2007). “Emplacement of a silicic lava dome through a crater glacier: Mount St Helens, 2004–06”. *Annals of Glaciology* 45, pages 14–20. DOI: [10.3189/172756407782282426](https://doi.org/10.3189/172756407782282426).

- Walter, T. R., C. E. Harnett, N. Varley, D. V. Bracamontes, J. Salzer, E. U. Zorn, M. Bretón, R. Arámbula, and M. E. Thomas (2019). “Imaging the 2013 explosive crater excavation and new dome formation at Volcán de Colima with TerraSAR-X, time-lapse cameras and modelling”. *Journal of Volcanology and Geothermal Research* 369, pages 224–237. DOI: [10.1016/j.jvolgeores.2018.11.016](https://doi.org/10.1016/j.jvolgeores.2018.11.016).
- Walter, T. R., E. U. Zorn, C. E. Harnett, A. V. Shevchenko, A. Belousov, M. Belousova, and M. S. Vassileva (2022). “Influence of conduit and topography complexity on spine extrusion at Shiveluch volcano, Kamchatka”. *Communications Earth & Environment* 3(1). DOI: [10.1038/s43247-022-00491-w](https://doi.org/10.1038/s43247-022-00491-w).
- Wang, T., M. P. Poland, and Z. Lu (2015). “Dome growth at Mount Cleveland, Aleutian Arc, quantified by time series TerraSAR-X imagery”. *Geophysical Research Letters* 42(24). DOI: [10.1002/2015gl066784](https://doi.org/10.1002/2015gl066784).
- Wang, T. and M. Bebbington (2012). “Estimating the likelihood of an eruption from a volcano with missing onsets in its record”. *Journal of Volcanology and Geothermal Research* 243–244, pages 14–23. DOI: [10.1016/j.jvolgeores.2012.06.032](https://doi.org/10.1016/j.jvolgeores.2012.06.032).
- Watts, R. B., R. A. Herd, R. S. J. Sparks, and S. R. Young (2002). “Growth patterns and emplacement of the andesitic lava dome at Soufrière Hills Volcano, Montserrat”. *The Eruption of Soufrière Hills Volcano, Montserrat, from 1995 to 1999*. Edited by T. H. Druitt and B. P. Kokelaar. Volume 21. 1. Geological Society of London, pages 115–152. ISBN: 1862390983. DOI: [10.1144/gsl.mem.2002.021.01.06](https://doi.org/10.1144/gsl.mem.2002.021.01.06).
- Wolpert, R. L., S. E. Ogburn, and E. S. Calder (2016). “The longevity of lava dome eruptions”. *Journal of Geophysical Research: Solid Earth* 121(2), pages 676–686. DOI: [10.1002/2015jb012435](https://doi.org/10.1002/2015jb012435).
- Závada, P., Z. Kratinová, V. Kusbach, and K. Schulmann (2009). “Internal fabric development in complex lava domes”. *Tectonophysics* 466(1–2), pages 101–113. DOI: [10.1016/j.tecto.2008.07.005](https://doi.org/10.1016/j.tecto.2008.07.005).
- Zeinalova, N., A. Ismail-Zadeh, O. Melnik, I. Tsepelev, and V. Zobin (2021). “Lava Dome Morphology and Viscosity Inferred From Data-Driven Numerical Modeling of Dome Growth at Volcán de Colima, Mexico During 2007–2009”. *Frontiers in Earth Science* 9. DOI: [10.3389/feart.2021.735914](https://doi.org/10.3389/feart.2021.735914).
- Zharinov, N. A. and Y. V. Demyanchuk (2008). “The growth of an extrusive dome on Shiveluch Volcano, Kamchatka in 1980–2007: Geodetic observations and video surveys”. *Journal of Volcanology and Seismology* 2(4), pages 217–227. DOI: [10.1134/s0742046308040015](https://doi.org/10.1134/s0742046308040015).
- Zorn, E. U., N. Le Corvec, N. R. Varley, J. T. Salzer, T. R. Walter, C. Navarro-Ochoa, D. M. Vargas-Bracamontes, S. T. Thiele, and R. Arámbula Mendoza (2019). “Load Stress Controls on Directional Lava Dome Growth at Volcán de Colima, Mexico”. *Frontiers in Earth Science* 7. DOI: [10.3389/feart.2019.00084](https://doi.org/10.3389/feart.2019.00084).
- Zorn, E. U., T. R. Walter, M. J. Heap, and U. Kueppers (2020). “Insights into lava dome and spine extrusion using analogue sandbox experiments”. *Earth and Planetary Science Letters* 551, page 116571. DOI: [10.1016/j.epsl.2020.116571](https://doi.org/10.1016/j.epsl.2020.116571).